2007-11-06

Distinct Roles for Two G{alpha} G Interfaces in Cell Polarity Control by a Yeast Heterotrimeric G Protein

Shelly Catherine Strickfaden
University of Massachusetts Medical School

Et al.

Molecular Biology of the Cell
Vol. 19, 181–197, January 2008

Distinct Roles for Two Gα–Gβ Interfaces in Cell Polarity Control by a Yeast Heterotrimeric G Protein

Shelly C. Strickfaden and Peter M. Pryciak

Department of Molecular Genetics and Microbiology, University of Massachusetts Medical School, Worcester, MA 01605

Submitted April 27, 2007; Revised October 9, 2007; Accepted October 22, 2007
Monitoring Editor: Daniel Lew

Saccharomyces cerevisiae **mating pheromones trigger dissociation of a heterotrimeric G protein (Gαβγ) into Gα-guanosine triphosphate (GTP) and Gβγ. The Gβγ dimer regulates both mitogen-activated protein (MAP) kinase cascade signaling and cell polarization. Here, by independently activating the MAP kinase pathway, we studied the polarity role of Gβγ in isolation from its signaling role. MAP kinase signaling alone could induce cell asymmetry but not directional growth. Surprisingly, active Gβγ, either alone or with Gα-GTP, could not organize a persistent polarization axis. Instead, following pheromone gradients (chemotropism) or directional growth without pheromone gradients (de novo polarization) required an intact receptor–Gαβγ module and GTP hydrolysis by Gα. Our results indicate that chemoattractant-induced cell polarization requires continuous receptor–Gαβγ communication but not modulation of MAP kinase signaling. To explore regulation of Gβγ by Gα, we mutated Gβ residues in two structurally distinct Gα–Gβ binding interfaces. Polarity control was disrupted only by mutations in the N-terminal interface, and not the Switch interface. Incorporation of these mutations into a Gβ–Gα fusion protein, which enforces subunit proximity, revealed that Switch interface dissociation regulates signaling, whereas the N-terminal interface may govern receptor–Gαβγ coupling. These findings raise the possibility that the Gαβγ heterotrimer can function in a partially dissociated state, tethered by the N-terminal interface.**

INTRODUCTION

Cell polarization involves the asymmetric distribution of intracellular materials in a way that is usually directed toward localized instructional cues, which can be internal or external to the cell. External cues govern chemotaxis in cells such as *Dictyostelium discoideum* and mammalian neutrophils, such that a gradient of chemoattractant from a localized source stimulates cell polarization and directed cell movement along the gradient (Iijima *et al*., 2002; Bagorda *et al*., 2006; Franca-Koh *et al*., 2006). The ability to coordinate the direction of cell movement with the location of the external signal implies that the initial sensing of chemoattractant and at least some of the subsequent intracellular signal transduction events do not occur uniformly within the cell but instead occur in an asymmetric, spatially restricted manner.

The mating reaction of the budding yeast *Saccharomyces cerevisiae* provides a model system to study how cells generate an asymmetric response to polarization stimuli. Here, the two haploid cell types (**a** or α) secrete cell type-specific mating pheromones (**a** factor or α factor, respectively), which serve as chemoattractants that stimulate mating responses in cells of the opposite type (Dohlman and Thorner, 2001). Each pheromone binds a specific G protein-coupled receptor (GPCR) (Ste2 or Ste3, which recognize α factor and **a** factor, respectively) that couples to a heterotrimeric G protein (Gαβγ, composed of Gpa1 [Gα], Ste4 [Gβ], and Ste18 [Gγ]), which is not cell type specific. Binding of pheromone to the receptor catalyzes exchange of guanosine triphosphate (GTP) for guanosine diphosphate (GDP) on the Gα subunit, causing dissociation of Gα-GTP from the Gβγ dimer. Once released from the inhibitory Gα subunit, Gβγ can trigger signaling through a mitogen-activated protein (MAP) kinase cascade; this involves membrane recruitment of the scaffold protein Ste5, which leads to activation of the Ste5-associated kinases, Ste11 (MAP kinase kinase kinase), Ste7 (MAP kinase kinase), and Fus3 (MAP kinase [MAPK]) (Pryciak and Huntress, 1998; Mahanty *et al*., 1999; van Drogen *et al*., 2000, 2001; Winters *et al*., 2005). These signaling events induce cell cycle arrest and the transcription of mating specific genes (Dohlman and Thorner, 2001).

Mating pheromones also regulate cell morphology. The actin cytoskeleton and membrane trafficking systems are rearranged to form a polarized mating projection, which then grows toward the partner in a process termed chemotropism (Segall, 1993; Arkowitz, 1999; Pruyne and Bretscher, 2000). These polarization events highlight another role for Gβγ. Current evidence suggests that Gβγ recruits the polarity proteins Far1 and Cdc24 (Valtz *et al*., 1995; Butty *et al*., 1998; Nern and Arkowitz, 1998, 1999) to the region of plasma membrane receiving the highest pheromone dose. Cdc24 is the guanine-nucleotide exchange factor (GEF) for the Rho-family GTPase Cdc42, which controls actin organization and cell polarity (Chant, 1999; Etienne-Manneville, 2004). Far1 is an adaptor protein that binds both Gβγ and Cdc24 (Butty *et al*., 1998; Nern and Arkowitz, 1999). Hence, communication between Gβγ and Far1/Cdc24 is thought to direct Cdc42 activity to the proper site to allow polarized growth along the gradient of pheromone. This process may be facilitated

This article was published online ahead of print in *MBC in Press* (http://www.molbiolcell.org/cgi/doi/10.1091/mbc.E07–04–0385) on October 31, 2007.

Address correspondence to: Peter M. Pryciak (peter.pryciak@umassmed.edu).

by additional interactions between Gα and Fus3 (Metodiev *et al*., 2002) or between Gβγ and Rho1 (Bar *et al*., 2003).

For chemotactic cells (*Dictyostelium* and neutrophils) and chemotropic cells (yeast), a gradient of chemoattractant normally serves as a spatial cue for the direction of polarization. However, these cells will still polarize when exposed to a uniform concentration of chemoattractant, implying the existence of "symmetry breaking" mechanisms that can generate asymmetric responses to symmetric signals (Sohrmann and Peter, 2003; Wedlich-Soldner and Li, 2003). In yeast, prior work reveals two ways in which a cell can polarize when pheromone is provided uniformly rather than as a gradient, which we will refer to as "default" and "de novo" polarization. Default polarization uses preexisting polarity information provided by the bud site selection proteins as a spatial cue, resulting in the formation of a mating projection at the presumptive bud site (Madden and Snyder, 1992; Dorer *et al*., 1995; Nern and Arkowitz, 1999). This default polarization is independent of Far1–Cdc24 communication, but it depends on bud site selection proteins such as Rsr1/Bud1 (Nern and Arkowitz, 1999). When these default sites are absent, cells can still polarize in a uniform field of pheromone, but now the axis of polarization forms de novo at random positions that bear no relationship to previous polarization sites. This de novo polarization is independent of bud site selection proteins, but it requires Far1–Cdc24 binding; when this binding is disrupted, cells initiate polarization but fail to organize a stable axis of polarized growth (Nern and Arkowitz, 1999, 2000). Thus, interactions that are required for asymmetric response to a gradient of pheromone are also required when asymmetric growth is initiated de novo.

To better understand how external signals couple with intracellular factors to generate an asymmetric response, we investigated the regulation of yeast Gβγ activity in response to a gradient or uniform field of pheromone. We show that in addition to Gβγ, the receptor and Gα are required not only to sense pheromone gradients during chemotropism but also for directionally persistent growth during de novo polarization. In addition, by using a series of mutations in Gβ (Ste4) to disrupt regulation of Gβγ by Gα, we observed qualitatively different polarity phenotypes depending on which Gα-Gβ interaction interface is disrupted. Our results suggest that one Gα–Gβ interface controls signaling, whereas the other facilitates directional responses by allowing receptor–Gαβγ coupling.

MATERIALS AND METHODS

Yeast Strains

Yeast strains are listed in Table 1. P_{GAL1}-*STE5ΔN-CTM* was integrated at the *HIS3* locus by transformation with NheI-digested pPP1268 to create strains PPY1303, PPY1304, PPY1306, and PPY1307. P_{GAL1}-*STE11ΔN-STE7* was integrated at the *HIS3* locus by transformation with NheI-digested pPP1270 to create strains PPY1309, PPY1310, PPY1311, PPY1312, PPY1313, PPY1314, PPY1951, and PPY1952.

Plasmids

Plasmids used in this study are listed in Table 2. Ste4 mutants defective at binding Gpa1 (see next section) were originally isolated as variants of the two-hybrid construct pPP268 (identical to pGAD-STE4 except for an extra SphI site following *STE4*) and then were transferred as EcoRI–BamHI fragments to a two-hybrid construct with a stronger promoter, pGADXP-STE4. All mutations were also transferred into pPP2968 (CEN *URA3 STE4*) as PstI–XhoI or BglII–BsaI (for W411R) fragments; pPP2968 contains *STE4* on a 2.4-kb AflII–BspHI fragment cloned into blunted XbaI and XhoI sites of a derivative of pRS316 in which the *URA3* gene lacks a PstI site. Mutations causing the most severe disruption of Gpa1–Ste4 binding (i.e., K126E, L117R, W136R L138F, and L154R N156K) were also moved to other contexts for further study. First, they were transferred as MscI–XhoI fragments from the pPP268 derivatives into the P_{GAL1}-*STE4* construct pGT-STE4 (Klein *et al*., 2000). Then, the mutants were placed under control of the native *STE4* promoter by transferring MscI–BspEI fragments from these P_{GAL1}-*STE4* constructs into pPP1340. In addition, the mutations were transferred as MscI–XhoI fragments into a P_{GAL1}-*STE4-GPA1* fusion construct pSTE4-GPA1-b (Klein *et al*., 2000). These *STE4–GPA1* fusions were then placed under control of the native *STE4* promoter by transferring MscI–BspEI fragments from the P_{GAL1}-*STE4–GPA1* fusion constructs into pPP226, which contains *STE4* on a 4-kb EcoRI fragment, from −2045 to +2003, in the EcoRI site of pRS316.

To construct *STE4–GPA1* fusions harboring the *GPA1-Q323L* mutation, the Q323L mutation was first transferred on a SphI–SphI fragment from pRS316-GPA1-Q323L (Apanovitch *et al*., 1998) into the *STE4–GPA1* fusion construct pPP1340, creating pPP1859. Then, the BglII–BspEI fragment from pPP1859 was transferred into pPP1343 to create pPP2801. To place these mutant *STE4–GPA1* fusions under control of the *GAL1* promoter, the MscI–BspEI fragments from pPP1859 and pPP2801 were transferred into pSTE4-GPA1-b (Klein *et al*., 2000), creating pPP2806 and pPP2807.

Plasmid pPP2711 (CEN *TRP1 GPA1*) was created by polymerase chain reaction (PCR) amplification of *GPA1* (−201 to +1707) and ligation as a SacI–KpnI fragment into pRS314 (Sikorski and Hieter, 1989). The *GPA1* mutations Q323L and K21E R22E were transferred into pPP2711 as BsrGI–BstBI fragments from pRS316-GPA1-Q323L (Apanovitch *et al*., 1998) and YCplac22-GPA1-K21ER22E (Metodiev *et al*., 2002), to create pPP2802 and pPP2743, respectively. The *GPA1* mutations E28K and E28A were generated by site-directed mutagenesis of YCpGPA1 (Stone and Reed, 1990) and pPP247 (Pryciak and Hartwell, 1996), creating plasmids pPP1501, pPP1502, pPP1503, and pPP1505. The P_{GAL1}-*STE7* construct pPP2773 was made by transferring *STE7* as a BamHI–PstI fragment from pG7 (Harris *et al*., 2001) into the CEN *TRP1* P_{GAL1} vector pPP449 (Pryciak and Huntress, 1998).

To create epitope-tagged forms of Ste4 and Gpa1, we first introduced unique NotI sites into their coding sequences. For *STE4*, the NotI site was added between a repeat of the first two codons (ATG GCA agc ggc cgc ATG GCA), and then a myc_{13} NotI–NotI cassette was inserted to create pPP2838 (myc_{13}-*STE4*) and pPP2839 (myc_{13}-*STE4-GPA1* fusion). Although these derivatives were functional in vivo, the myc_{13} epitope caused reduced signaling in *FUS1-lacZ* and halo assays, and thus they were used only to test effects of Ste4 mutations on protein levels and Gpa1 coimmunoprecipitation. For *GPA1*, intact N and C termini of the protein are functionally important. Hence, the NotI site was added within a yeast-specific insert region (Lambright *et al*., 1996), overlapping codons 161–163 (AgC GGc CGc) and introducing a conservative residue change (T161S). An HA_3 NotI–NotI cassette was then inserted, creating pPP2775. These derivatives were fully functional in vivo.

Isolation of Ste4 Mutants

1. A genetic screen was conducted using a two-hybrid assay to isolate Ste4 mutants with specific defects in binding Gpa1. Libraries of *ste4* mutants (made by error-prone PCR) were created in a two-hybrid activation-domain vector (pGAD424) as described previously (Pryciak and Hartwell, 1996), and they were transformed into a *MAT***a** two-hybrid reporter strain (L40). Transformants were mated by replica plating to a *MATα* strain (AMR70) harboring DNA-binding domain (DBD) fusions to either Gpa1 (pBTM-GPA1) or Ste18 (pBTM-STE18). Clones were identified that showed reduced interaction with Gpa1 but not with Ste18. Secondary screens tested interaction with Ste5 (pM276p16) and Far1 (pPP743). All sequenced isolates harbored mutations in residues that contact Gα in crystal structures (Lambright *et al*., 1996; Sondek *et al*., 1996). These isolates (and their mutations) were as follows: Gm3-E41 (L154S), Gm3-C7 (K126E), Gm5-B47 (K126E D370G), Gm5-E73 (L117R), Gm4-H32 (D224V), Gm4-J38 (D224E D402E), and Gm4-I22 (S164W K213R D272A V375A). The D272A mutation in Gm4-I22 was separated from the other mutations by swapping restriction fragments; although largely responsible for the Gpa1-binding defect, the single D272A mutant was not as severe as the original quadruple mutant, and therefore all assays reported here for D272A used the stronger quadruple mutant. The isolate Gm3-E41 (L154S) was briefly reported previously (Pryciak and Hartwell, 1996). Because this L154S mutant did not show the strong chemotropism defects seen with N-terminal interface mutants (see *Results*), and because both Leu154 and the neighboring Asn156 residue are predicted to contact Gpa1 (Lambright *et al*., 1996; Sondek *et al*., 1996), we made an additional mutant (L154R N156K) in an attempt to cause a more severe disruption. In fact, this mutant and the original L154S mutant were effectively indistinguishable, and so only the mutant with the more-drastic substitution (L154R N156K) is analyzed here. In addition, for comparison to the phenotypically strong mutants L117R and K126E, we made less drastic substitutions at the same positions (L117A, L117G, K126A, K126N).
2. Another screen was designed to isolate Ste4 mutants with reduced mating efficiency but normal pathway signaling. A *ste4* mutant library was created in a P_{GAL1} vector (pYES-R) as described previously (Pryciak and Hartwell, 1996), and it was transformed into a *MAT***a** *ste4Δ FUS1-lacZ* strain. Transformants were mated (on galactose medium) to a mixed lawn of pheromone-producing and pheromoneless *MATα* cells, and screened for clones showing reduced mating only with the pheromone-

Table 1. Yeast strains used in this study

Strain background[a]	Strain name	Genotype	Source
(a)	PPY498	*MAT***a** *FUS1::FUS1-lacZ::LYS2 fus3::LEU2 kss1::ura3^{FOA}*	This study
(a)	PPY577	*MAT***a** *FUS1::FUS1-lacZ::LYS2 ADE3*	This study
(a)	PPY662	*MAT***a** *FUS1::FUS1-lacZ::LYS2 ste4::ura3^{FOA}*	This study
(a)	PPY663	*MAT***a** *FUS1::FUS1-lacZ::LYS2*	Strickfaden *et al.* (2007)
(a)	PPY817	*MAT***a** *FUS1::FUS1-lacZ::LYS2 far1::ADE2*	Strickfaden *et al.* (2007)
(a)	PPY820	*MAT***a** *FUS1::FUS1-lacZ::LYS2 fus3::LEU2 kss1::ura3^{FOA} far1::ADE2*	This study
(a)	PPY824	*MAT***a** *FUS1::FUS1-lacZ::LYS2 fus3::LEU2*	This study
(a)	PPY827	*MAT***a** *FUS1::FUS1-lacZ::LYS2 fus3::LEU2 far1::ADE2*	This study
(a)	PPY836	*MAT***a** *HIS4 far1::ADE2*	This study
(b)	PPY398	*MAT***a**	Harris *et al.* (2001)
(b)	PPY794	*MAT***a** *ste4::ura3^{FOA}*	Pryciak and Huntress (1998)
(b)	PPY842	*MAT***a** *ste4::ura3^{FOA} ste5::ADE2 ste20-1::TRP1*	Winters *et al.* (2005)
(b)	PPY856	*MAT***a** *FUS1::FUS1-lacZ::LEU2 ste4::ura3^{FOA}*	Winters *et al.* (2005)
(b)	PPY858	*MAT***a** *FUS1::FUS1-lacZ::LEU2 ste5::ADE2*	Pryciak and Huntress (1998)
(b)	PPY863	*MAT***a** *ste5::ADE2 ste20-1::TRP1*	This study
(b)	PPY867	*MAT***a** *ste4::ura3^{FOA} ste5::ADE2*	This study
(b)	PPY886	*MAT***a** *FUS1::FUS1-lacZ::LEU2 ste5::ADE2 ste4::ura3^{FOA}*	Pryciak and Huntress (1998)
(b)	PPY978	*MAT***a** *FUS1::FUS1-lacZ::LEU2 ste5::ADE2 gpa1::URA3*	This study
(b)	PPY979	*MAT***a** *FUS1::FUS1-lacZ::LEU2 ste5::ADE2 ste2::URA3*	This study
(b)	PPY989	*MAT***a** *FUS1::FUS1-lacZ::LEU2 ste5::ADE2 ste18::URA3*	This study
(b)	PPY1228	*MAT***a** *ste4::ura3^{FOA} gpa1::ura3^{FOA}*	This study
(b)	PPY1230	*MAT***a** *ste4::ura3^{FOA} gpa1::ura3^{FOA} ste5::ADE2*	This study
(b)	PPY1248	*MAT***a** *ste4::ura3^{FOA} rsr1::ura3::HIS3*	This study
(b)	PPY1259	*MAT***a** *rsr1::ura3::HIS3*	This study
(b)	PPY1303	*MAT***a** *HIS3::P_{GAL1}-STE5ΔN-CTM*	This study
(b)	PPY1304	*MAT***a** *HIS3::P_{GAL1}-STE5ΔN-CTM ste5::ADE2*	This study
(b)	PPY1306	*MAT***a** *HIS3::P_{GAL1}-STE5ΔN-CTM rsr1::URA3*	This study
(b)	PPY1307	*MAT***a** *HIS3::P_{GAL1}-STE5ΔN-CTM rsr1::URA3 ste5::ADE2*	This study
(b)	PPY1309	*MAT***a** *HIS3::P_{GAL1}-STE11ΔN-STE7*	This study
(b)	PPY1310	*MAT***a** *HIS3::P_{GAL1}-STE11ΔN-STE7 ste5::ADE2*	This study
(b)	PPY1311	*MAT***a** *HIS3::P_{GAL1}-STE11ΔN-STE7 ste5::ADE2 ste4::ura3^{FOA}*	This study
(b)	PPY1312	*MAT***a** *HIS3::P_{GAL1}-STE11ΔN-STE7 rsr1::URA3*	This study
(b)	PPY1313	*MAT***a** *HIS3::P_{GAL1}-STE11ΔN-STE7 rsr1::URA3 ste5::ADE2*	This study
(b)	PPY1314	*MAT***a** *HIS3::P_{GAL1}-STE11ΔN-STE7 rsr1::URA3 ste5::ADE2 ste4::ura3^{FOA}*	This study
(b)	PPY1380	*MAT***a** *gpa1::ura3^{FOA} ste4::ura3^{FOA} rsr1::ura3^{FOA}*	This study
(b)	PPY1662	*MAT***a** *FUS1::FUS1-lacZ::LEU2 ste4::ura3^{FOA} ste7::ADE2*	This study
(b)	PPY1663	*MAT***a** *FUS1::FUS1-lacZ::LEU2 ste4::ura3^{FOA} gpa1::ura3^{FOA}*	This study
(b)	PPY1937	*MAT***a** *fus3::LEU2 ste4::ura3^{FOA}*	This study
(b)	PPY1942	*MAT***a** *ste4::ura3^{FOA} gpa1::ura3^{FOA} sst2::LEU2*	This study
(b)	PPY1951	*MAT***a** *HIS3::P_{GAL1}-STE11ΔN-STE7 ste5::ADE2 gpa1::ura3^{FOA}*	This study
(b)	PPY1952	*MAT***a** *HIS3::P_{GAL1}-STE11ΔN-STE7 ste5::ADE2 gpa1::ura3^{FOA} rsr1::URA3*	This study
(c)	AMR70	*MATα URA3::(lexAop)$_8$-lacZ lys2 met2*	Hollenberg *et al.* (1995)
(c)	L40	*MAT***a** *LYS2::(lexAop)$_4$-HIS3 URA3::(lexAop)$_8$-lacZ*	Hollenberg *et al.* (1995)
(c)	PPY762	*MAT***a** *LYS2::(lexAop)$_4$-HIS3 URA3::(lexAop)$_8$-lacZ ste11::ADE2*	Butty *et al.* (1998)
(c)	PPY1158	*MAT***a** *LYS2::(lexAop)$_4$-HIS3 ura3^{FOA}::(lexAop)$_8$-lacZ ste11::ADE2 gpa1::URA3*	This study
(d)	PT2α	*MATα hom3 ilv1 can1*	Pryciak and Huntress (1998)

[a] Strain background: (a) 381G (*cry1 ade2-1^{oc} ade3 his4-580^{am} leu2-3,112 lys2^{oc} trp1^{am} ura3-52 SUP4-3^{ts}*). (b) W303 (*ade2-1 his3-11,15 leu2-3,112 trp1-1 ura3-1 can1*). (c) S288c (*ade2 his3-Δ200 leu2-3,112 trp1-901*). (d) Other.

producing *MATα* partner. The same clones were also screened for intact *FUS1-lacZ* induction (on galactose plates), by using a filter-based β-galactosidase assay (Bartel and Fields, 1995). Five isolates with the strongest mating defects were sequenced. One had multiple mutations and was not pursued further. Each of the others harbored mutations at Lys126 (three were K126E, one was K126N). One isolate, called m3-D10 (T76S K126E) was described previously (Pryciak and Hartwell, 1996). Because their mutations and phenotypes were similar to other K126E mutants (see 1), further analysis of these isolates is not presented.

3. A Ste4 mutant with Gpa1-binding defects, W136R L138F, which was isolated in a previous screen (Whiteway *et al*., 1994), was also studied here. This mutation was transferred by PCR from its original context (CEN *HIS3 P_{GAL1}-STE4$^{Hpl\ 21–1}$*) into pPP268, and then it was transferred to other contexts in parallel with the new mutations.
4. Site-directed mutagenesis was used to target Ste4 residues that were predicted to contact Gpa1 but that were not uncovered in unbiased screens. Structural data predict that Gα is contacted by 16 Gβ residues that lie in nine regions (Lambright *et al*., 1996; Sondek *et al*., 1996). The mutations identified from genetic screens (see 1–3) affected six of these nine regions. Therefore, the other three regions (composed of 6 residues) were mutated, using drastic residue changes to disrupt Gpa1 binding as severely as possible. These included the triple mutation N92G K94E S96A, the double mutation T181R Y183N, and the single mutation W411R. The T181R Y183N mutant was defective in all assays, and it was defective at binding all partners tested (including Ste18), suggesting it may be misfolded, and so it was not pursued further. The other mutations had only weak effects on Gpa1 binding (see *Results*), consistent with their absence from genetic screens.
5. Additional mutants used as controls were isolated in screens for Ste4 mutants with Ste18-binding defects (e.g., Gm3-F30 [D97G K380E]) (Pryciak and Hartwell, 1996) or with defects in binding Ste5 and Far1 (e.g., Gm3-J70 [L49P]). The D97G K380E mutation disrupts binding to the Gγ subunit Ste18 and hence to Gβγ-binding partners; each mutation lies close to a predicted Gγ-contact residue (W100 and L379) (Sondek *et al*., 1996), although it is not known which mutation disrupts Ste18 binding (or whether both contribute). The L49P mutant was isolated in a screen to be described elsewhere, but it harbors a mutation identical to a mutation found previously (Dowell *et al*., 1998).

Table 2. Plasmids used in this study

Name	Alias	Description	Source
pPP120	pRD-STE11-H3	CEN URA3 P_{GAL1}-GST-STE11ΔN	Neiman and Herskowitz (1994)
pPP126	YCpGPA1	CEN LEU2 GPA1	Stone and Reed (1990)
pPP134	pNC252	2 μm URA3 P_{GAL1}-STE12	Pryciak and Hartwell (1996)
pPP226[a]	p316-ST4-a	CEN URA3 P_{STE4}-STE4 (-2045 to +2003)	This study
pPP244	pGAD424	2 μm LEU2 GAL4-AD vector	Bartel and Fields (1995)
pPP247	pBTM-GPA1	2 μm TRP1 lexA-DBD-GPA1	Pryciak and Hartwell (1996)
pPP249	pGAD-STE4	2 μm LEU2 GAL4-AD-STE4	Pryciak and Hartwell (1996)
pPP255	pBTM-STE18	2 μm TRP1 lexA-DBD-STE18	Pryciak and Hartwell (1996)
pPP268[a]	pGAD-YS4	2 μm LEU2 GAL4-AD-STE4 (w/extra SphI site)	This study
pPP271	pGS12-T	2 μm TRP1 P_{GAL1}-STE12	This study
pPP305	pM276p16	2 μm TRP1 lexA-DBD-STE5(1-214)	Whiteway *et al.* (1995)
pPP446	pRD53-2 μm	2 μm URA3 P_{GAL1} vector	This study
pPP452	pGS5	CEN TRP1 P_{GAL1}-STE5	Pryciak and Huntress (1998)
pPP473	pGS5ΔN-CTM	CEN TRP1 P_{GAL1}-ste5ΔN-CTM (= Snc2 TM domain)	Pryciak and Huntress (1998)
pPP479	pH-GS5ΔN-CTM	CEN HIS3 P_{GAL1}-ste5ΔN-CTM (= Snc2 TM domain)	Pryciak and Huntress (1998)
pPP513	pGFP-GS5ΔN-CTM	CEN TRP1 P_{GAL1}-GFP-ste5ΔN-CTM (= Snc2 TM domain)	Pryciak and Huntress (1998)
pPP524	pGFP-GS5ΔN-SEC22	CEN TRP1 P_{GAL1}-GFP-ste5ΔN-Sec22 TM domain	Pryciak and Huntress (1998)
pPP575	pGS11ΔN-T	CEN TRP1 P_{GAL1}-GST-STE11ΔN	Moskow *et al.* (2000)
pPP636	pGADXP	2 μm LEU2 strong P_{ADH1}-GAL4-AD vector	Butty *et al.* (1998)
pPP643[a]	pGADXP-STE4	2 μm LEU2 strong P_{ADH1}-GAL4-AD-STE4	Butty *et al.* (1998)
pPP679	pRS314	CEN TRP1 vector	Sikorski and Hieter (1989)
pPP681	pRS316	CEN URA3 vector	Sikorski and Hieter (1989)
pPP741	pNC252-HIS3	2 μm HIS3 P_{GAL1}-STE12	This study
pPP743	pBTM-FAR1 174-285	2 μm TRP1 lexA-DBD-FAR1(174-285)	This study
pPP854	p3058	CEN LEU2 P_{FUS1}-lacZ reporter	Roberts *et al.* (2000)
pPP1150[a]	pSTE4-GPA1-b	CEN URA3 P_{GAL1}-STE4-GPA1 fusion (1 a.a. linker)	Klein *et al.* (2000)
pPP1151[a]	pGT-STE4	CEN URA3 P_{GAL1}-STE4	Klein *et al.* (2000)
pPP1175	pH-GFP-GS5ΔN-SEC22	CEN HIS3 P_{GAL1}-GFP-ste5ΔN-Sec22 TM domain	This study
pPP1268	pIH-GS5ΔN-CTM	integrating HIS3 P_{GAL1}-ste5ΔN-CTM (= Snc2 TM domain)	This study
pPP1270	pIH-G11ΔN.S7	integrating HIS3 P_{GAL1}-STE11ΔN-STE7 fusion	This study
pPP1340[a]	pS4GA-WT	CEN URA3 P_{STE4}-STE4-GPA1 fusion	This study
pPP1501	YCpGPA1-E28K	CEN LEU2 GPA1(E28K)	This study
pPP1502	pBTM-GPA1-E28K	2 μm TRP1 lexA-DBD-GPA1(E28K)	This study
pPP1503	YCpGPA1-E28A	CEN LEU2 GPA1(E28A)	This study
pPP1505	pBTM-GPA1-E28A	2 μm TRP1 lexA-DBD-GPA1(E28A)	This study
pPP1621	YCplac22-GPA1-WT	CEN TRP1 GPA1	Stratton *et al.* (1996)
pPP2711	p314-GPA1-WT	CEN TRP1 GPA1	This study
pPP2743	p314-GPA1-K21ER22E	CEN TRP1 GPA1(K21E R22E)	This study
pPP2773	pRS314-G7	CEN TRP1 P_{GAL1}-STE7	This study
pPP2775	p314-GPA1-HA-M	CEN TRP1 HA_3-GPA1	This study
pPP2802	p314-GPA1-Q323L	CEN TRP1 GPA1(Q323L)	This study
pPP2838[a]	p316P*-mycS4	CEN URA3 P_{STE4}-myc_{13}-STE4	This study
pPP2839[a]	p316P*-mycS4GA-WT	CEN URA3 P_{STE4}-myc_{13}-STE4-GPA1 fusion	This study
pPP2968[a]	p316P*-ST4AB	CEN URA3 P_{STE4}-STE4 (-780 to +1616)	This study

a.a., amino acids; TM, transmembrane.

[a] These plasmids, containing wild-type *STE4*, serve as the parental constructs for multiple mutant derivatives used in this study encompassing 71 additional plasmids, which consist of 15 mutant derivatives each of pPP268 and pPP643, 13 derivatives of pPP2968, six derivatives each of pPP1150 and pPP1340, and four derivatives each of pPP226, pPP1151, pPP2838, and pPP2839.

Microscopy

For de novo and default polarization assays, transformants were grown in selective raffinose media, and expression of P_{GAL1}-driven constructs was induced by addition of galactose to 2%; where indicated, 10 μM α factor was also added simultaneously. After 2- to 8-h induction, cells were visualized without fixation. Differential labeling of old and new cell surface growth with fluorophore-conjugated concanavalin A (ConA) used methods described previously (Nern and Arkowitz, 2000; Matheos *et al.*, 2004). Cells were grown first in synthetic raffinose medium, labeled with 0.1 mg/ml fluorescein isothiocyanate (FITC)-ConA, induced with 2% galactose ± 10 μM α factor for 4 h, and then labeled with 0.05 mg/ml tetramethylrhodamine B isothiocyanate (TRITC)-ConA.

Mating Assays

For patch mating assays, **a** cells were patched directly onto a lawn of partner PT2α cells, mated overnight at 30°C, and then diploids were selected by replication to minimal media. After an immediate (1°) replica was made, more dilute replicas were made by repeating the replication of the master mating plate twice more, using a fresh velvet each time, to create 2° and 3° replicas (Harris *et al.*, 2001). Replicas were incubated for 2 d at 30°C. For pheromone confusion assays, α factor was spread on one plate to give a final concentration of 30 μM (unless indicated otherwise) and allowed to dry before the PT2α lawn was spread.

Quantitative mating assays followed previous methods (Pryciak and Huntress, 1998; Lamson *et al.*, 2002). In brief, plasmid-transformed cells were grown overnight in selective raffinose medium, and then 0.5–5 × 10^6 **a** cells were mixed with an equal number of wild-type α cells (strain PT2α) and collected onto filters. The filters were placed on SC/raffinose/galactose plates and incubated for 6–7 h (unless indicated otherwise) at 30°C. Afterward, filters were suspended in phosphate-buffered saline (PBS), and serial dilutions were plated on minimal media to select for diploids. Mating efficiency was calculated as the percentage of input haploid cells (before mating) that formed diploid colonies (after mating). Where indicated, α factor was spread on the mating plate (to give a final concentration of 30 μM) before filters were added.

To analyze zygote formation, mated cells were suspended in PBS, sonicated, and fixed in 5% formaldehyde. Cells were imaged by differential

interference contrast microscopy (DIC) and green fluorescent protein (GFP) microscopy.

Pheromone Response, β-Galactosidase, and Two-Hybrid Assays

Halo assays of growth arrest were performed by plating cells on −Trp-Ura plates and overlaying with filters containing 20 μl of 1 mM α factor (Lamson *et al*., 2002). Plates were incubated for 2 d at 30°C.

FUS1-lacZ transcriptional induction assays were performed as described previously (Pryciak and Huntress, 1998; Lamson *et al*., 2002). Induction by pathway-activating constructs under control of the *GAL1* promoter was measured 4 h after addition of 2% galactose ± 10 μM α factor to cultures grown in raffinose medium. For *FUS1-lacZ* assays comparing mutant derivatives of P_{GAL1}-*STE4* in *ste4*Δ cells, or *STE4* derivatives in *ste4*Δ *ste7*Δ + P_{GAL1}-*STE7* cells, cultures in raffinose medium were pretreated with 2% galactose for 1 h and then treated for 2 h with 2% galactose ± 10 μM α factor.

β-Galactosidase and two-hybrid assays were performed as described previously (Pryciak and Hartwell, 1996; Lamson *et al*., 2002).

Cell Lysates and Protein Analysis

To test coimmunoprecipitation of myc_{13}-Ste4 with HA_3-Gpa1, clarified cell lysates were prepared by glass bead lysis, incubated with mouse anti-myc (9E10; Santa Cruz Biotechnology, Santa Cruz, CA) or mouse anti-hemagglutinin (HA) (HA.11; Covance Research Products, Princeton, NJ) antibodies and precipitated with protein G-agarose beads by using methods described previously (Lamson *et al*., 2002). After separation by SDS-polyacrylamide gel electrophoresis (PAGE) and transfer to polyvinylidene difluoride membranes, blots were probed with rabbit anti-myc (A-14; Santa Cruz Biotechnology) or rabbit anti-HA (HA.11; Covance Research Products). To analyze steady-state levels of Ste4 and Ste4-Gpa1 fusion proteins, crude whole-cell extracts were prepared by pelleting 1.5 ml of culture (OD_{660} = 0.5), resuspension in 45 μl of SDS-PAGE loading buffer supplemented with protease inhibitors (Lamson *et al*., 2002), and boiling for 10 min. After pelleting cell debris for 2 min, 10 μl was analyzed by SDS-PAGE, blotted, and probed with rabbit anti-myc (A-14; Santa Cruz Biotechnology).

RESULTS

Separating the Polarity Role of Gβγ from Its Signaling Role

The Gβγ dimer normally performs two roles in the mating pathway: it activates MAP kinase cascade signaling and it regulates proteins that control cell polarity. Our goal in this work was to study the polarity role of the receptor–Gαβγ module in isolation from its requirement in activating the MAP kinase cascade. Therefore, we used a variety of methods to activate signaling independent of pheromone and Gβγ, and then studied how perturbing Gαβγ function affects chemotropism and cell polarization. This strategy is an extension of one used previously in which overexpression of the transcription factor Ste12 was used to study the mating role of various MAP kinase pathway components while bypassing their role in transcriptional induction (Schrick *et al*., 1997). Here, we used several newer reagents such as membrane-targeted versions of Ste5 (Ste5ΔN-CTM and Ste5ΔN-Sec22), which can promote robust MAP kinase cascade signaling, wild-type levels of mating, and normal polarized morphogenesis (Pryciak and Huntress, 1998; Harris *et al*., 2001). To ensure that communication between Gβγ and Ste5 was severed, these reagents used a truncated form of Ste5 that lacks the Gβγ-binding site (Ste5ΔN), and all assays were performed in strains where the genomic *STE5* locus was deleted (*ste5*Δ). For comparison, we also used a constitutively active form of Ste11 (Ste11ΔN) (Cairns *et al*., 1992; Neiman and Herskowitz, 1994) and overexpressed Ste12 (Dolan and Fields, 1990; Schrick *et al*., 1997). When signaling output was measured by induction of a transcriptional reporter construct (*FUS1-lacZ*), we found that some bypass methods caused stronger activation than others, but all were independent of Ste4 (Gβ) and pheromone (Figure 1A, right).

We then used these signaling bypass methods to address the role of Gβγ in chemotropic mating. Chemotropism was monitored using a "pheromone confusion" assay (Dorer *et al*., 1995; Nern and Arkowitz, 1998), in which mating success is compared in the absence versus presence of excess exogenously added pheromone (α factor), which obscures natural pheromone gradients emanating from partner cells. Chemotropically proficient cells can use pheromone gradients to locate mating partners, and thus they mate with higher efficiency when pheromone gradients are left intact (−α factor) than when gradients are obscured (+α factor); cells defective at chemotropism cannot follow pheromone gradients, and thus they mate at the lower efficiency under either condition. Thus, this assay does not directly monitor directional growth, but rather it infers the ability of cells to detect and use pheromone gradients. Unlike earlier measures of "mating partner discrimination" (Jackson and Hartwell, 1990; Jackson *et al*., 1991), chemotropic proficiency in the pheromone confusion assay requires both Far1 and Far1–Cdc24 binding (Dorer *et al*., 1995; Valtz *et al*., 1995; Nern and Arkowitz, 1998), and it accurately reflects the ability of cells to establish a new polarization axis along pheromone gradients (Valtz *et al*., 1995; Nern and Arkowitz, 1998). Using this assay, we found that cells expressing Ste4 were proficient at chemotropism, whereas those lacking Ste4 were defective (Figure 1A, left). Among the different bypass methods, the membrane-targeted Ste5 reagents promoted the most efficient mating, but a consistent behavior emerged regardless of the bypass method or the absolute signaling level; namely, removal of Ste4 or addition of excess pheromone disrupted chemotropic mating without altering MAP kinase pathway signaling.

Gβγ activates MAP kinase cascade signaling via interactions with Ste5 and Ste20 (Whiteway *et al*., 1995; Inouye *et al*., 1997; Feng *et al*., 1998; Leeuw *et al*., 1998; Pryciak and Huntress, 1998). To unequivocally determine whether these interactions are dispensable for the chemotropic role of Gβγ, we performed quantitative assays of chemotropic mating in *ste5*Δ *ste20*Δ cells, by using activated Ste11 (Ste11ΔN) or excess Ste12 to induce signaling or transcription. Indeed, these cells were proficient at chemotropism, whereas strains that also lacked Ste4 (*ste4*Δ *ste5*Δ *ste20*Δ) were not (Figure 1B). Thus, the chemotropism role of Gβγ does not require it to interact with Ste5 or Ste20. These findings provided a framework from which to further probe the chemotropism and polarity functions of the receptor–Gαβγ module without concern for their effects on MAP kinase pathway signaling.

The Pheromone Receptor and All Three Gαβγ Subunits Are Required for Chemotropism

The ability of Gβγ to mediate chemotropism without regulating MAP kinase cascade signaling is consistent with the fact that Gβγ interacts directly with polarity proteins via Far1 (Butty *et al*., 1998; Nern and Arkowitz, 1998, 1999). However, because chemotropism is a directional phenomenon, it would be logical that Gβγ–Far1 binding could help guide polarization in the proper direction only if Gβγ was activated in a spatially asymmetric manner, congruent with the pheromone gradient. Because Gβγ activation is regulated by the receptor and Gα subunit, we directly compared the requirement for the receptor and all three G protein subunits in chemotropic mating assays. As mentioned above, MAP kinase signaling, transcription, or both were activated independent of Gβγ, so that genetic perturbation of the receptor–Gαβγ module would affect only chemotropism. We found that only the cells with an intact receptor–Gαβγ module could use pheromone gradients to increase

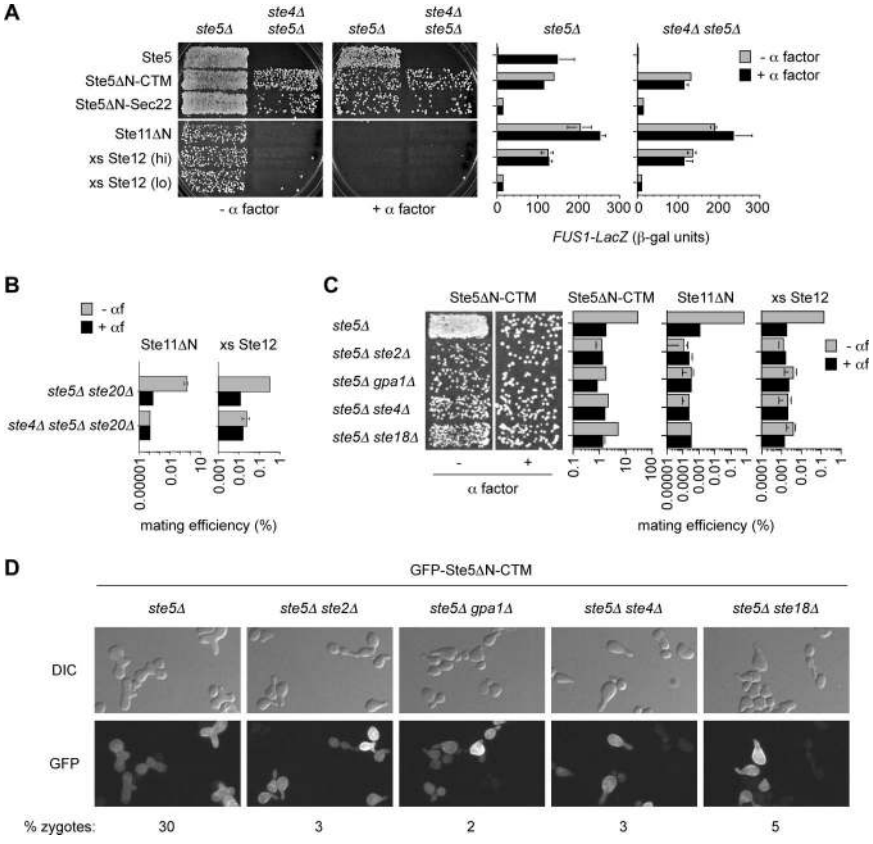

Figure 1. Chemotropism role of G$\alpha\beta\gamma$ and receptor is separate from signaling. (A) Chemotropism requires Ste4 even when its signaling role is bypassed. Strains PPY858 (*ste5*Δ) and PPY886 (*ste5*Δ *ste4*Δ) harbored galactose-inducible forms of Ste5 (pPP452), Ste5ΔN-CTM (pPP513), Ste5ΔN-Sec22 (pPP524), Ste11ΔN (pPP575), or Ste12 (pPP741 or pPP271). Chemotropic proficiency (left) was assessed by patch matings performed in the absence (−) or presence (+) of exogenous α factor. The mating results using Ste5 derivatives show the more-dilute 2° replica, whereas the others show the 1° replica (see *Materials and Methods*). Results were similar in both **a** and α cells, and in both W303 and 381G strain backgrounds (unpublished observations). Transcriptional activation of *FUS1-lacZ* (right) is shown for the same strains and plasmids after galactose induction ± α factor. Bars, mean ± SD (n = 3). To emphasize that transcription levels were not the primary determinant of mating efficiency, results are shown using Ste12 overexpression constructs that yield high (hi) or low (lo) levels of transcriptional induction (due to different vector contexts). (B) Ste4 can perform its chemotropism role without Ste5 and Ste20. Quantitative matings were performed ± exogenous α factor. Strains PPY863 and PPY842 harbored galactose-inducible Ste11ΔN (pRD-STE11-H3) or Ste12 (pNC252). Bars, mean ± range (n = 2). (C) An intact receptor–G$\alpha\beta\gamma$ module is required for chemotropism. Signaling was activated by galactose-inducible constructs (pPP513, pPP575, and pPP741) in the indicated strains (PPY858, PPY979, PPY978, PPY886, and PPY989). Chemotropism was monitored by patch or quantitative mating assays in the absence (−) or presence (+) of α factor. Bars, mean ± SD (for Ste5ΔN-CTM; n = 4) or mean ± range (n = 2). Transcriptional activation of *FUS1-lacZ* by the same constructs after galactose induction ± α factor was similar in all strains (data not shown). (D) Zygote formation. Strains from C, harboring galactose-inducible GFP-Ste5ΔN-CTM (pPP513), were mated with PT2α partner cells for 5.5 h. Representative fields of DIC and fluorescence (GFP) images are shown. We counted 500 cells for each mixture, and the percentage that were zygotes is shown.

their mating success, whereas cells lacking the receptor (*ste5*Δ *ste2*Δ) or any one of the G protein subunits (*ste5*Δ *gpa1*Δ, *ste5*Δ *ste4*Δ, or *ste5*Δ *ste18*Δ) could not (Figure 1C). It is important to note that under these signaling bypass conditions the receptor–G$\alpha\beta\gamma$ module can only contribute to mating success when pheromone gradients are intact, whereas it performs no detectable role when gradients are absent (i.e., the wild-type and null alleles of each component are indistinguishable).

Microscopic analysis (Figure 1D) confirmed that the intact receptor–G$\alpha\beta\gamma$ module allowed cells to locate and fuse with mating partners, as judged by the formation of dumbbell-shaped zygotes, although the mating-defective cells could still form polarized mating projections. Therefore, under these conditions the receptor-G$\alpha\beta\gamma$ module is not required for polarization per se, but for properly guiding cell polarization toward a mating partner. Note that these findings are consistent with the expectation that polarization in the "correct" direction (i.e., toward the source of pheromone) should require spatial regulation of G$\beta\gamma$ activity, and so they do not necessarily imply that the receptor and/or Gα perform separate polarization functions.

Free G$\beta\gamma$ Is Insufficient for De Novo Polarization

To study the polarity function of the receptor–G$\alpha\beta\gamma$ module in a setting where cells do not have to detect the direction of a localized stimulus, we assayed de novo polarization in response to a uniform field of pheromone. Polarization was restricted to the de novo pathway by using *rsr1*Δ mutant strains, in which the default pathway is inactivated (Nern and Arkowitz, 1999, 2000). First, we tested whether pheromone had a role in de novo polarization beyond activating the MAP kinase cascade. Pathway signaling was activated by expressing either Ste5ΔN-CTM (P_{GAL1}-*STE5*Δ*N-CTM*) or an activated form of Ste11 fused to Ste7 (P_{GAL1}-*STE11*Δ*N-STE7*), which permits normal mating morphology by reducing cross-activation of other signaling pathways (Harris *et al*., 2001). Despite being able to trigger default polarization (i.e., in *RSR1* cells), pathway activation by Ste5ΔN-CTM or Ste11ΔN-Ste7 could not trigger de novo polarization (i.e., in *rsr1*Δ cells) (Figure 2A). This inability was not due to interference from excess MAP kinase pathway signaling, as cells harboring these activators (*ste5*Δ + P_{GAL1}-*STE5*Δ*N-CTM* or P_{GAL1}-*STE11*Δ*N-STE7*) could undergo de novo polarization when pheromone was added (Figure 2B). Importantly, we found that de novo polarization requires G$\beta\gamma$ activity, as cells lacking the Gβ subunit (*ste4*Δ *ste5*Δ + P_{GAL1}-*STE11*Δ*N-STE7*) did not polarize even when pheromone was added (Figure 2B). Notably, however, communication between G$\beta\gamma$ and Ste5 was not required, because pheromone could stimulate polarization in cells lacking Ste5 (*ste5*Δ + P_{GAL1}-*STE11*Δ*N-STE7*) (Figure 2B). As expected, transcriptional

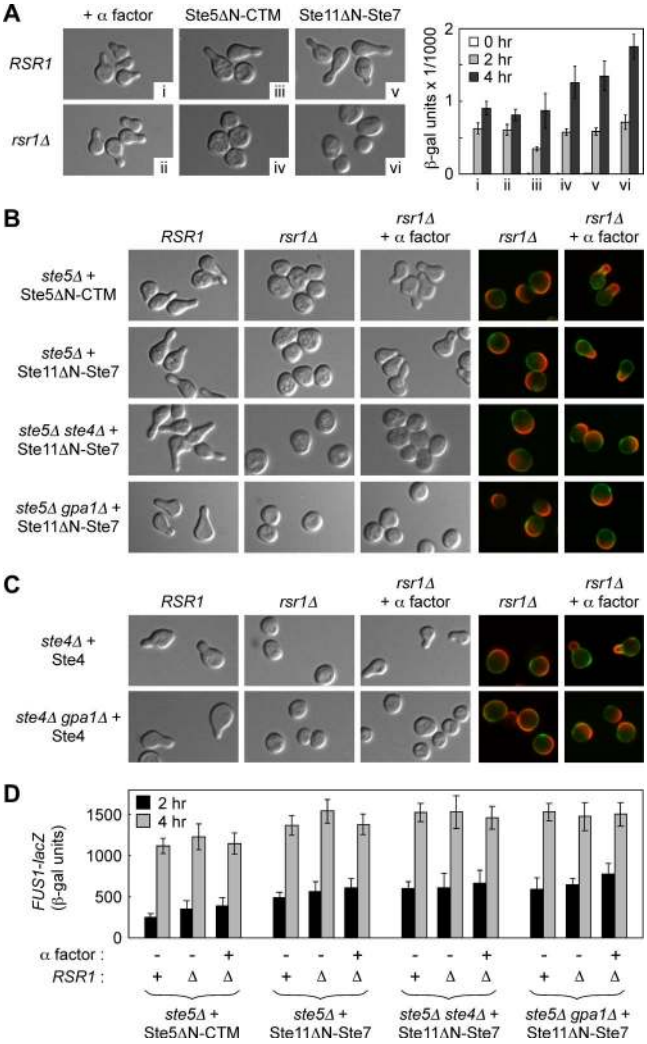

Figure 2. De novo polarization requires pheromone and Gα, in addition to Gβγ. (A) Polarization was examined in *RSR1* or *rsr1*Δ cells, after signaling was activated by α factor (strains PPY398 and PPY1259) or by galactose induction of P_{GAL1}-*STE5*Δ*N-CTM* (strains PPY1303 and PPY1306) or P_{GAL1}-*STE11*Δ*N-STE7* (strains PPY1309 and PPY1312). Right, the same strains were transformed with a *FUS1-lacZ* reporter (p3058), and transcriptional induction (mean ± SD; n = 4) was monitored 0, 2, and 4 h after addition of galactose with (i and ii) or without (iii–vi) α factor. (B) Pheromone, Ste4, and Gpa1 are required for de novo polarization. The indicated *rsr1*Δ strains harboring P_{GAL1}-*STE5*Δ*N-CTM* or P_{GAL1}-*STE11*Δ*N-STE7* (PPY1307, PPY1313, PPY1314, and PPY1952) were treated with galactose ± α factor. Congenic *RSR1* strains (PPY1304, PPY1310, PPY1311, and PPY1951) show that the galactose-inducible constructs can activate polarization by the default pathway. Right, old cell wall was labeled with FITC-ConA (green), and new cell wall formed during the period of mating pathway activation was labeled with TRITC-ConA (red). (C) Free Gβγ is not sufficient for de novo polarization. Strains PPY794, PPY1228, PPY1248, and PPY1380 harboring P_{GAL1}-*STE4* (pGT-STE4) were induced with galactose ± α factor. At right, old and new cell wall was labeled as in B. (D) Conditions affecting de novo polarization do not affect transcription. The eight strains in B were transformed with reporter plasmid p3058, and *FUS1-lacZ* induction (mean ± SD; n = 4) was monitored 2–4 h after addition of galactose ± α factor.

induction levels and kinetics in these strains were uninfluenced by the factors that governed polarization, such as *RSR1*, *STE4*, or pheromone (Figure 2, A and D). Therefore, as with chemotropism, the ability of pheromone and Gβγ to regulate de novo polarization is separable from any regulatory effects on the MAP kinase cascade.

Because de novo polarization does not require cells to sense the direction from which pheromone emanates, and because Gβγ interacts directly with Far1 and Cdc24, (Butty *et al*., 1998; Nern and Arkowitz, 1998, 1999), it seemed possible that Gβγ alone would be sufficient to promote de novo polarization, with pheromone serving only to generate free Gβγ by dissociating the Gαβγ heterotrimer. To test this view, Gβγ was activated without using pheromone, by deletion of *GPA1* or by overexpression of *STE4* (P_{GAL1}-*STE4*). To avoid persistent growth arrest due to constitutive MAP kinase pathway signaling, *GPA1* was deleted in a *ste5*Δ strain harboring P_{GAL1}-*STE11*Δ*N-STE7* (Figure 2B) or in a *ste4*Δ strain harboring P_{GAL1}-*STE4* (Figure 2C). Remarkably, although each method of Gβγ activation (i.e., *gpa1*Δ or P_{GAL1}-*STE4*) could induce cell cycle arrest and cell polarization by the default pathway (i.e., in *RSR1* cells), neither method could induce de novo polarization (i.e., in *rsr1*Δ cells) (Figure 2, B and C). Furthermore, the ability of pheromone to trigger de novo polarization was actually eliminated by the *gpa1*Δ mutation (Figure 2, B and C, right columns), and thus it requires Gα in addition to Gβγ. Therefore, although Gβγ can directly communicate with polarization proteins, free Gβγ is not sufficient for de novo polarization. This deficiency might reflect a separate role for ligand-bound receptors or GTP-loaded Gα, or it might indicate that receptors and Gα can promote an asymmetric distribution of Gβγ activity even when external pheromone is distributed uniformly.

To follow the pattern of cell surface growth, we used fluorophore-conjugated ConA to differentially label cell wall formed before versus during the period of mating pathway activation. It was previously shown that when de novo polarization failed due to disruption of Far1–Cdc24 interaction, cells could initiate polarized growth, but the polarization axis could not be maintained; consequently, it wandered about a broad region of the cell periphery (Nern and Arkowitz, 2000). Similarly, we observed that when cells failed de novo polarization due to absence of pheromone, Gpa1, or Ste4, they still showed asymmetric cell surface growth, but it was broadly distributed across one hemisphere (Figure 2, B and C, right). Thus, consistent with the requirement for Fus3 (Matheos *et al*., 2004), our results suggest that activation of the MAP kinase cascade is sufficient to initiate asymmetric growth, even in the absence of Gα or Gβγ. Nevertheless, organization of a well-focused and persistent polarization axis requires both Far1–Cdc24 interaction and an intact receptor–Gαβγ module.

Gβ Mutants Reveal Distinct Roles for Two Gα–Gβ Binding Interfaces

To further investigate the requirement for the intact receptor–Gαβγ module in chemotropism and de novo polarization, we used a series of Gβ mutants to disrupt regulation of Gβγ by the Gα subunit. Crystal structures of mammalian Gαβγ heterotrimers reveal two contact surfaces between Gα and Gβ, termed the "switch interface" and the "N-terminal interface" (Wall *et al*., 1995; Lambright *et al*., 1996). The switch (Sw) interface involves a region of Gα that undergoes a conformational switch upon GTP binding, whereas the N-terminal (Nt) interface involves an N-terminal helix of Gα that protrudes away from the globular GTPase domain (Figure 3A). The Gα and Gβ residues contacting one another in each interface are well conserved between mammalian and yeast counterparts (Lambright *et al*., 1996; Sondek *et al*.,

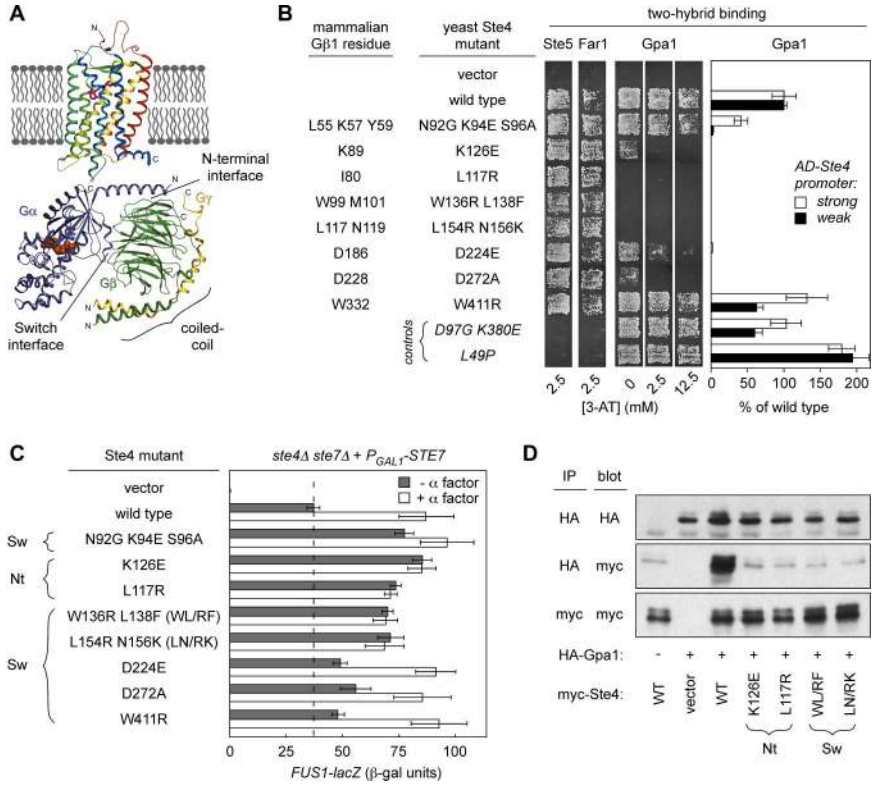

Figure 3. Ste4 mutations in Gα–Gβ binding interfaces. (A) Model for orientation of the G protein-coupled receptor rhodopsin, the heterotrimeric G protein transducin, and the membrane. Adapted from Hamm, 2001; copyright *Proceedings of the National Academy of Sciences USA*. (B) Effects of Ste4 mutations on Gpa1 binding. Mutated Ste4 residues are listed alongside their homologous residues in mammalian Gβ1. Activation domain fusions (AD-Ste4) were expressed in a *gpa1*Δ *ste11*Δ two-hybrid tester strain (PPY1158), with DNA-binding domain fusions to Gpa1 (pPP247) or to the G$\beta\gamma$-binding regions of Ste5 (pPP305) or Far1 (pPP743). Binding was detected by growth on −His plates ± 3-aminotriazole (3-AT; an inhibitor of His3), or by quantitative β-galactosidase assay (bars, mean ± SD; n = 4). To reveal the full range of effects on Gpa1 binding, quantitative assays used AD–Ste4 fusions expressed from either a strong promoter (derivatives of pPP643) or a weak promoter (derivatives of pPP268); plate growth assays used pPP643 derivatives. As controls (at bottom), two additional Ste4 mutations outside the Gα–Gβ interfaces (see *Materials and Methods*) were analyzed in parallel; these disrupt binding to Ste5 and Far1, but not to Gpa1. (C) Ste4 mutations cause deregulated signaling. To avoid constitutive growth arrest, the Ste4 mutants were tested in *ste4*Δ *ste7*Δ cells (PPY1662) harboring P_{GAL1}-*STE7* (pPP2773). *FUS1-lacZ* induction (mean ± SD; n = 4) was measured 2 h after addition of galactose ± α factor. Ste4 was expressed from the native *STE4* promoter (derivatives of pPP2968; vector = pRS316). (D) Ste4 mutations disrupt coimmunoprecipitation with Gpa1. HA-tagged Gpa1 (pPP2775) or vector (pRS314) was coexpressed with myc-tagged Ste4 (derivatives of pPP2838; vector = pRS316) in strain PPY1230 (*gpa1*Δ *ste4*Δ *ste5*Δ). Cell extracts were analyzed by immunoprecipitation (IP) and immunoblotting (blot).

1996); in Gβ these include 16 residues in nine regions. Here, we studied a series of Ste4 (Gβ) mutations that collectively affect all positions predicted to contact Gα. These mutants were derived from multiple sources; briefly, mutations in six of the nine Gα-contact regions were identified in three different genetic screens, and the remaining regions were changed by site-directed mutagenesis (see *Materials and Methods*).

By a two-hybrid assay (Figure 3B), the Ste4 mutations identified in genetic screens reduced Gpa1 binding to levels that were either undetectable (L117R, W136R L138F, and L154R N156K) or extremely faint (K126E, D224E, and D272A), whereas site-directed mutations at the remaining positions (N92G K94E S96A and W411R) had only mild effects (suggesting why they were not identified in screens). A similar rank order of defects was seen using a coprecipitation assay of these AD–Ste4 fusions with Gpa1-GST (unpublished observations). In comparison, these mutations had minimal effects on interaction with Ste5 and Far1 (Figure 3B); this is consistent with our findings (to be described in detail elsewhere) that binding to Ste5 and Far1 requires Ste4 (Gβ) and Ste18 (Gγ) residues in the coiled-coil region of the G$\beta\gamma$ dimer (Lamson and Pryciak, unpublished observations), which has been previously implicated in downstream signaling (Leberer *et al*., 1992; Grishin *et al*., 1994a,b; Leeuw *et al*., 1998; Winters *et al*., 2005). As expected for mutants released from repression by Gpa1, these Ste4 mutants caused constitutively active pathway signaling (Figure 3C), although some mutants that retained detectable Gpa1 binding also showed incomplete deregulation, because signaling could still be increased by α factor. Therefore, we focused most of our subsequent studies on four Ste4 mutants with the strongest Gpa1-binding defects and the most deregulated signaling, which include two in the Nt interface (L117R and K126E) and two in the Sw interface (W136R L138F and L154R N156K, hereafter termed WL/RF and LN/RK, respectively). These mutations did not affect Ste4 protein levels but they eliminated detectable coimmunoprecipitation with Gpa1 (Figure 3D).

Despite similar behavior in binding and signaling assays, mutations in the two Gα–Gβ interfaces had opposite effects on polarity control. Mutations in the Nt interface disrupted chemotropism, because the cells were largely insensitive to the presence or absence of pheromone gradients (Figure 4A). This phenotype is consistent with deregulated G$\beta\gamma$ activity. Surprisingly, however, the Sw interface mutants were chemotropism proficient (Figure 4A), even though by signaling and binding criteria they seemed to be as strongly dissociated from Gpa1 as the Nt interface mutants. Although it was possible that the individual Sw mutations have a less disruptive effect on Gpa1 interaction than the Nt mutations, two further observations suggested that the explanation was not this simple. First, chemotropism remained intact even when multiple Sw interface mutations were combined, such as W136R L138F L154R N156K (WL/RF + LN/RK; Figure 4A), as well as D224V D272A, L154S D272A, and W136R L138F D272A (unpublished observations). Second, by making less drastic substitutions at Nt interface residues (i.e., K126A, K126N, L117A, and L117G), we could detect residual Gpa1 binding for several of these new mutants (as well as the original K126E); yet, they all showed a stronger defect in

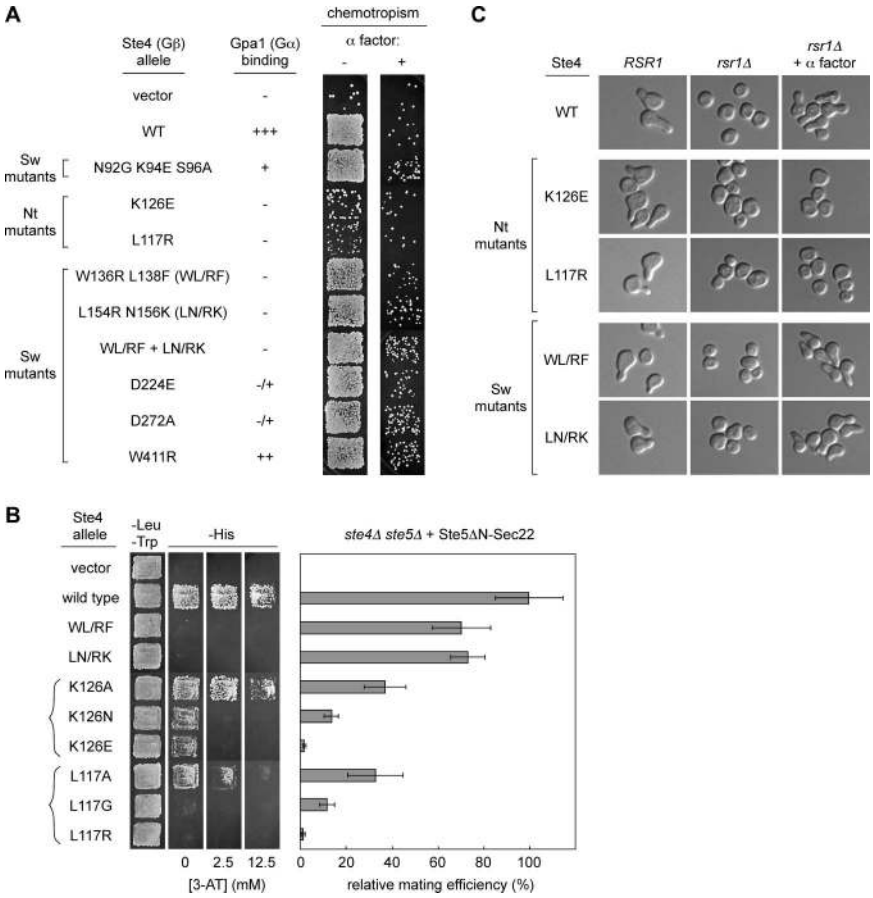

Figure 4. Ste4 mutations in the Nt interface, but not the Sw interface, disrupt polarity control. (A) Chemotropism proficiency was assessed by patch mating assays performed in the absence (−) or presence (+) of exogenous α factor. PPY867 (*ste4*Δ *ste5*Δ) harbored P_{GAL1}-*STE5*Δ*N-SEC22* (pPP524) and either vector (pRS316) or Ste4 variants expressed from the native *STE4* promoter (derivatives of pPP2968). The effects of the Ste4 mutations on Gpa1 binding are summarized for reference (see Figure 3B). (B) Analysis of additional Nt interface mutants. Left, two-hybrid binding assays (as in Figure 3B) using AD–Ste4 fusions (derivatives of pPP643; vector=pPP636) and DBD-Gpa1 (pPP247) in PPY1158. (Note: in quantitative assays using the lacZ reporter, the Gpa1 interaction signal of Ste4-K126A was measurably reduced to 27% of Ste4-WT.) Right, quantitative assays of Ste4 function during chemotropic mating. PPY867 (*ste4*Δ *ste5*Δ) harbored P_{GAL1}-*STE5*Δ*N-SEC22* (pPP524) and either vector (pRS316) or Ste4 variants (derivatives of pPP2968). As Ste4 affects mating under these conditions only when gradients are intact (see Figures 1, A–C, and 4A), these assays were conducted only in the absence of exogenous α factor. Results (mean ± SD; n = 4) were normalized to the average mating efficiency of wild-type Ste4. (C) Default and de novo polarization phenotypes. To avoid constitutive growth arrest, Ste4 mutants were expressed from the *GAL1* promoter (derivatives of pPP1151) in PPY794 (*ste4*Δ *RSR1*) or PPY1248 (*ste4*Δ *rsr1*Δ), and cell morphology was examined after induction with galactose ± α factor.

chemotropic mating than the Sw mutants WL/RF and LN/RK (Figure 4B).

The Ste4 mutants also segregated into two phenotypic classes in de novo polarization assays, in which the Sw interface mutants remained competent, whereas the Nt interface mutants were defective (Figure 4C, *rsr1*Δ). Notably, although the Sw interface mutants could mediate de novo polarization, they still required the addition of pheromone, as with wild-type Ste4. Thus, the Sw interface mutants remain capable of mediating a pheromone-dependent step, despite their strong dissociation from Gpa1 in binding and signaling assays. This raised the possibility that the Sw interface mutants can maintain a weak interaction between Gα and Gβ at the Nt interface (perhaps only when membrane-associated) and thus remain in regulatory communication with the pheromone receptor. This scenario, and others, was addressed by further experiments described below.

Suppression of an Nt Interface Mutant by a Compensatory Mutation in Gα

First, we wanted to determine whether the stronger phenotype of the Nt mutants was truly a consequence of disrupted interaction between Gβ and Gα, rather than between Gβ and some other protein involved in cell polarity. Although these Ste4 mutants could still bind Far1 (Figure 3B), in principle we could not rule out effects on binding to other, unknown partners. Therefore, we attempted to restore Gα–Gβ binding via a compensatory mutation in Gpa1. One of the Nt interface mutations (Ste4-K126E) involves a residue that, based on mammalian Gαβγ structures, is expected to form an ion pair between Lys126 in Ste4 and Glu28 in Gpa1 (Figure 5A). The Ste4 mutation changes Lys126 to Glu (K126E), thereby reversing the charge. To make a compensatory charge-reversal mutation in Gpa1, we changed Glu28 to Lys (E28K). This Gpa1–E28K mutation, but not a control mutation (Gpa1-E28A), restored measurable binding with Ste4-K126E (Figure 5B), although not to wild-type levels. Also, the Gpa1 E28K and E28A mutations each reduced binding to wild-type Ste4, although by a mild degree that was most noticeable when Ste4 was expressed at lower levels from a weak promoter (Figure 5B). It was not entirely surprising that Gpa1-E28K only partially restored binding to Ste4-K126E and that Ste4-K126E caused a stronger binding defect than Gpa1-E28K, because the mammalian Gβ residue homologous to Ste4 Lys126 contacts Gα not only through this ion pair but also through hydrogen bonding and van der Waals interactions (Lambright *et al.*, 1996). Nevertheless, these binding effects were enough to confer informative phenotypes in mating assays.

Indeed, the chemotropism defect of the Ste4-K126E mutant was at least partially suppressed by the Gpa1-E28K mutant, because mating of cells harboring Ste4-K126E was more efficient when coexpressed with Gpa1-E28K than with Gpa1-wild type (WT) (Figure 5, C and D). Whereas the Gpa1–E28K mutation reduced mating when combined with Ste4-WT, it increased mating by an average of 4.6-fold when combined with Ste4-K126E (Figure 5D). Although mating was not restored to wild-type levels, it would be unreasonable to expect this given the incomplete restoration of Gpa1–Ste4 binding. Notably, the observed suppression was allele-specific, because Gpa1-E28A did not suppress Ste4-K126E, and neither Gpa1-E28K nor Gpa1-E28A could suppress the

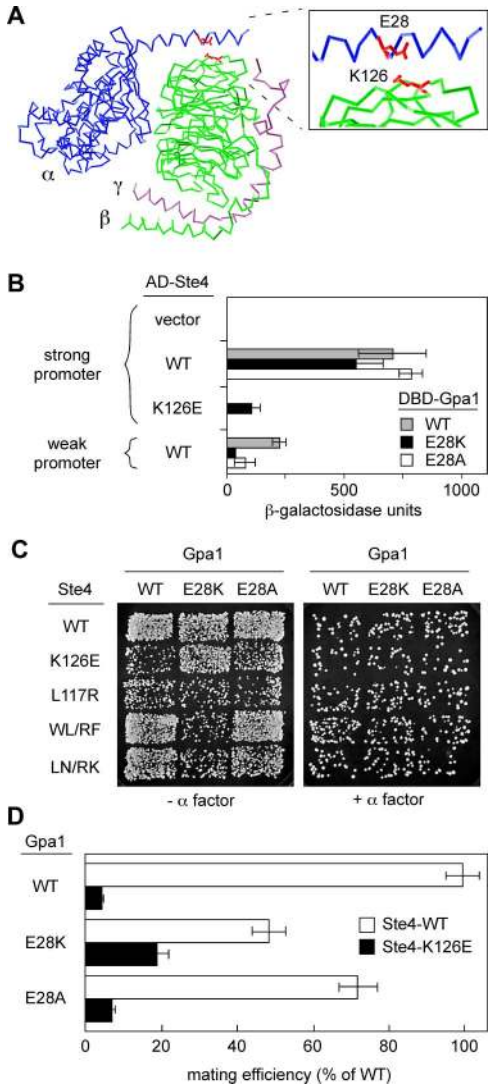

Figure 5. Allele-specific suppression of a Ste4 Nt interface mutant. (A) Red side chains highlight an ion pair predicted to form between Ste4(Gβ)-K126 and Gpa1(Gα)-E28 in the Nt interface, based on homologous residues (Gβ-K89 and Gα-E16) in transducin (Lambright *et al*., 1996). Structural rendering of G$\alpha\beta\gamma$ used Protein Data Bank coordinate set #1GOT and Cn3D version 4.1 software (National Center for Biotechnology Information/National Library of Medicine). (B) Two-hybrid assay showing that the Gpa1-E28K mutation partially restores interaction with Ste4-K126E. DBD fusions to Gpa1 derivatives (pPP247, pPP1502, and pPP1505) were coexpressed in PPY762 with AD–Ste4 fusions under control of either a strong or weak promoter (pPP636, pPP643, pPP1121, or pPP249). Bars, mean ± SD (n = 3). (C) Gpa1-E28K partially suppresses the chemotropism defect of Ste4-K126E. Patch mating assays used *ste4*Δ *gpa1*Δ *ste5*Δ cells (PPY1230) harboring P_{GAL1}-*STE5*Δ*N-SEC22* (pPP524) and the indicated combinations of *GPA1* (YCpGPA1, pPP1501, pPP1503), and *STE4* (derivatives of pPP226). (D) Quantitative mating assay measuring suppression of Ste4-K126E by Gpa1-E28K. Cells were as in panel C, mated to partner strain PT2α in the absence of exogenous α factor. Mating frequencies from eight independent 7-h mating experiments were expressed relative to the average of the fully wild-type combination (Gpa1-WT + Ste4-WT). Bars, mean ± SEM (n = 8). For Ste4-K126E matings, the difference between Gpa1-WT and Gpa1-E28K (means, 4.1 vs. 18.7%) was ranked highly significant ($p < 0.0005$) by a two-tailed unpaired Student's *t* test.

other Nt mutant, Ste4-L117R (Figure 5, C and D). Furthermore, although the Gpa1–E28K mutation improved mating by Ste4-K126E, it reduced mating by Ste4-WL/RF and Ste4-LN/RK, such that these Sw mutants were actually more defective than Ste4-K126E in cells expressing Gpa1-E28K (Figure 5C). This finding makes it highly unlikely that the phenotypic differences between Ste4 Nt and Sw mutations can be explained by their different impact on binding between G$\beta\gamma$ and an unknown factor. Instead, the pattern of allele-specific suppression and enhancement found with the Gpa1–E28K mutation supports a special role for Gα–Gβ binding via the Nt interface in chemotropism and cell polarization, and it suggests that this interface can remain functional when the Sw interface is dissociated by mutation. Because the Gpa1-E28K mutant is sensitized to disruption of the Sw interface, an intact Sw interface may help maintain Gα–Gβ association when the Nt interface is mildly disrupted.

Differences between Nt and Sw Interface Mutants Are Not Due to Altered Gpa1–Fus3 Interaction

Gpa1 can interact with the MAPK Fus3 via a docking motif in its N terminus, and mutations in this motif (Gpa1-K21E R22E, denoted Gpa1-EE) disrupt Fus3 binding and reduce mating (Metodiev *et al*., 2002). This raised the possibility that an intact Nt interface is required mainly to allow proper interaction between the Gpa1 N terminus and Fus3. To test this notion, we used the Gpa1-EE mutant to disrupt interaction between Gpa1 and Fus3, and we found that the Nt and Sw mutations in Ste4 still showed their characteristic phenotypic differences (Figure 6A). We also tested the Ste4 mutants in cells lacking Fus3 (*ste4*Δ *fus3*Δ). Here, mating by the Sw interface mutants was not as efficient as that of wild-type Ste4, but it was still more efficient than that of the Nt interface mutants (Figure 6A). Thus, both approaches suggest that the role of the Nt interface, and the different behavior of the Nt versus Sw mutants, cannot be explained by indirect effects on the Gpa1–Fus3 interaction.

It is notable that we did not detect a strong mating defect for the Gpa1-EE mutant alone, suggesting that the Gpa1–Fus3 interaction may not be required for chemotropism. To address this issue further, we compared the roles of Fus3 and Far1. Loss of either protein caused a mating defect, but a much greater defect occurred when both Fus3 and Far1 were absent (Figure 6B), indicating that although both proteins are required for maximum mating efficiency, each protein can perform its function without the other. Moreover, an important distinction between the roles of Fus3 and Far1 was apparent: the *fus3*Δ cells were proficient at chemotropism (i.e., sensitive to whether pheromone gradients were present or absent), whereas the *far1*Δ cells were defective (Figure 6B). To rule out the possibility that chemotropic proficiency in *fus3*Δ cells reflects redundancy between Fus3 and Kss1, we performed additional mating assays using *fus3*Δ *kss1*Δ cells (in which sterility was suppressed by P_{GAL1}-*STE12*). Despite low overall mating efficiency, the *fus3*Δ *kss1*Δ cells could still use pheromone gradients, and this behavior required Far1 (Figure 6C). The simplest overall interpretation is that detecting gradients and using gradient information to locate mating partners does not require Fus3, whereas the role of Fus3 in polarized morphogenesis (Matheos *et al*., 2004) is distinct from gradient sensing per se. These results also imply that, unlike cell cycle arrest (Gartner *et al*., 1998), phosphorylation of Far1 by Fus3 is dispensable for chemotropism.

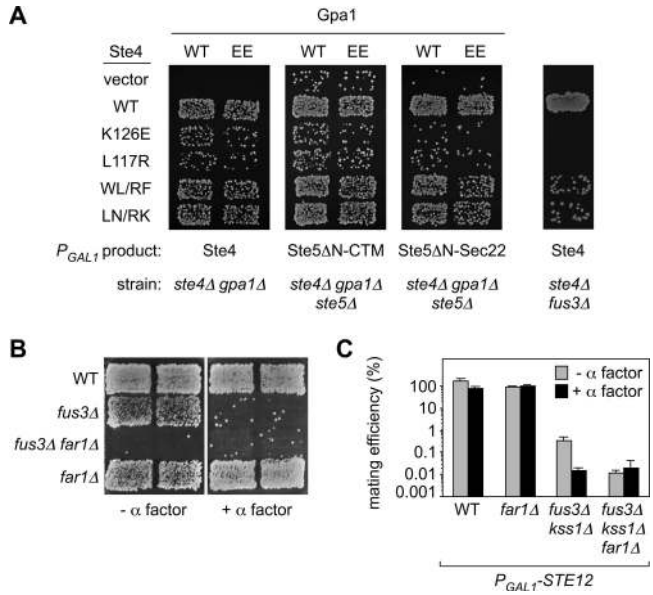

Figure 6. Qualitative differences between Ste4 Nt and Sw mutants are independent of Gpa1–Fus3 interaction. (A) Patch mating assays used the following strain and plasmid combinations. Left, strain PPY1228 (*ste4*Δ *gpa1*Δ) harbored the indicated Gpa1 derivatives (pPP2711 or pPP2743) and P_{GAL1}-*STE4* plasmids (derivatives of pPP1151). Center right, strain PPY1230 (*ste4*Δ *gpa1*Δ *ste5*Δ) harbored Gpa1 derivatives (pPP2711 or pPP2743) plus native *STE4* plasmids (derivatives of pPP226) and either P_{GAL1}-*STE5*Δ*N-CTM* (pPP479) or P_{GAL1}-*STE5*Δ*N-SEC22* (pPP1175). Far right, strain PPY1937 (*fus3*Δ *ste4*Δ) harbored the indicated P_{GAL1}-*STE4* plasmids. (B) Pheromone confusion assay showing that *fus3*Δ cells are chemotropically proficient. Strains, from top to bottom: PPY577, PPY824, PPY827, and PPY836. Similar results were also seen in S288C and W303 strain backgrounds (unpublished observations). (C) Quantitative mating assay of strains PPY663, PPY817, PPY498, and PPY820 expressing galactose-inducible Ste12 (pPP271). Cells were mated for 18 h, ± exogenous α factor. Bars, mean ± SD (n = 3).

Fusion of Gβ to Gα Suggests a Role for the Nt Interface in Receptor Coupling

Finally, we addressed whether maintenance of the Nt interface was necessary for coupling of the heterotrimer (Gαβγ) to the receptor. Existing models for the coupling between GPCRs and heterotrimeric G proteins predict that the Nt interface lies tangential to the membrane (Hamm, 1998, 2001). In addition, the N terminus of Gα has been implicated in receptor recognition (Taylor *et al*., 1994; Itoh *et al*., 2001; Cabrera-Vera *et al*., 2003). These facts suggested that the Nt interface mutations may not only disrupt interaction between Gβ and Gα, but they may also disrupt the way Gαβγ interacts with the receptor. However, the ability to test this notion was hindered by the fact that the Ste4 mutations caused constitutive signaling, which obscured whether the receptor might still exert some regulatory control over the G protein. To circumvent this difficulty, we took advantage of a previously described Ste4–Gpa1 fusion protein (Klein *et al*., 2000), with the rationale that forced association to Gpa1 may inhibit constitutive signaling by the Ste4 mutants and thus allow us to assay receptor coupling.

Starting with the prior Ste4–Gpa1 fusion construct, we replaced the original *GAL1* promoter with the native *STE4* promoter, and then compared its function with wild-type (unfused) polypeptides. By multiple assays, we found this Gβ–Gα fusion (Ste4-Gpa1) to function in a manner that was virtually indistinguishable from separate Gβ and Gα polypeptides. This included growth arrest (Figure 7A, left), regulation by the RGS-family protein Sst2 (Figure 7A, right), and pheromone-induced transcription (Figure 7B). Furthermore, the Gβ–Gα fusion was able to mediate total mating levels and chemotropic mating behavior that was similar to the wild-type heterotrimer (Figure 7, C and D). Thus, fusion of Gβ to Gα does not interfere with Gαβγ function in either signaling or gradient detection.

Next, we incorporated the Nt and Sw interface mutations into the *STE4* portion of the *STE4-GPA1* fusion gene (in both the *GAL1* promoter and native *STE4* promoter contexts), and we used *FUS1-lacZ* assays to determine whether forced association with Gpa1 could suppress the constitutive signaling activity of the Ste4 mutants. Again, the Nt interface and Sw interface mutants showed distinct phenotypes, but here it was the Sw interface mutants that were more strongly deregulated; that is, fusion to Gpa1 could squelch the constitutive signaling of the Nt interface mutants but not that of the Sw interface mutants (Figure 7E, left and middle). This suggests that dissociation of the Sw interface is the primary regulator of downstream signaling. There was a slight difference between the two Sw interface mutants in the native promoter context, because fusion to Gpa1 partially reduced signaling by Ste4-LN/RK but not Ste4-WL/RF (Figure 7E, top). Protein levels were unaffected by these mutations (Figure 7F).

Further analysis of these mutant fusion proteins showed that although constitutive signaling by the Nt interface mutants was suppressed by fusion to Gpa1, signaling could not be efficiently reactivated by the addition of pheromone, in contrast to the fusion containing wild-type Ste4 (Figure 7E, right). The feeble pheromone response suggests that mutations in the Nt interface disrupt coupling between Gαβγ and the receptor, which may explain their defective behavior in both chemotropism and de novo polarization assays. Thus, although both Sw and Nt mutants show constitutive signaling when not fused to Gpa1, their different behaviors when fused to Gpa1 suggest the possibility that their different chemotropism/polarity phenotypes are a consequence of disrupted receptor–Gαβγ coupling in the Nt mutants, and by inference that this coupling can still occur in Sw mutants despite their constitutive signaling.

GTP Hydrolysis by Gα Is Required for De Novo Polarization and Chemotropism

The findings described above suggest that proper communication between Gαβγ and the receptor is necessary for directionally persistent polarization even when the pheromone stimulus is provided uniformly. In theory, this receptor-Gαβγ communication could be required solely to promote GTP–GDP nucleotide exchange on Gα, perhaps allowing GTP-bound Gα to perform a polarization role that acts synergistically with Gβγ. Alternatively, receptor–Gαβγ communication might be required to generate asymmetry in the distribution of Gβγ activity (and/or Gα-GTP), which otherwise would remain symmetric (e.g., in *gpa1*Δ cells or with constitutively active Ste4 mutants). To address these possibilities, we used an activated mutant form of the Gα subunit, Gpa1-Q323L (herein referred to as Gpa1-QL), which is defective at GTP hydrolysis (Dohlman *et al*., 1996; Apanovitch *et al*., 1998). We found that simultaneous activation of both Gα and Gβγ, by coexpressing Gpa1-QL with Ste4, was still not sufficient for de novo polarization in the absence of pheromone (Figure 8, A and B). This was true regardless of whether Gpa1-QL was expressed with Ste4-WT or with the constitutively active Sw interface mutant, Ste4-WL/RF. In fact, we found that trapping Gpa1 in the GTP-bound state

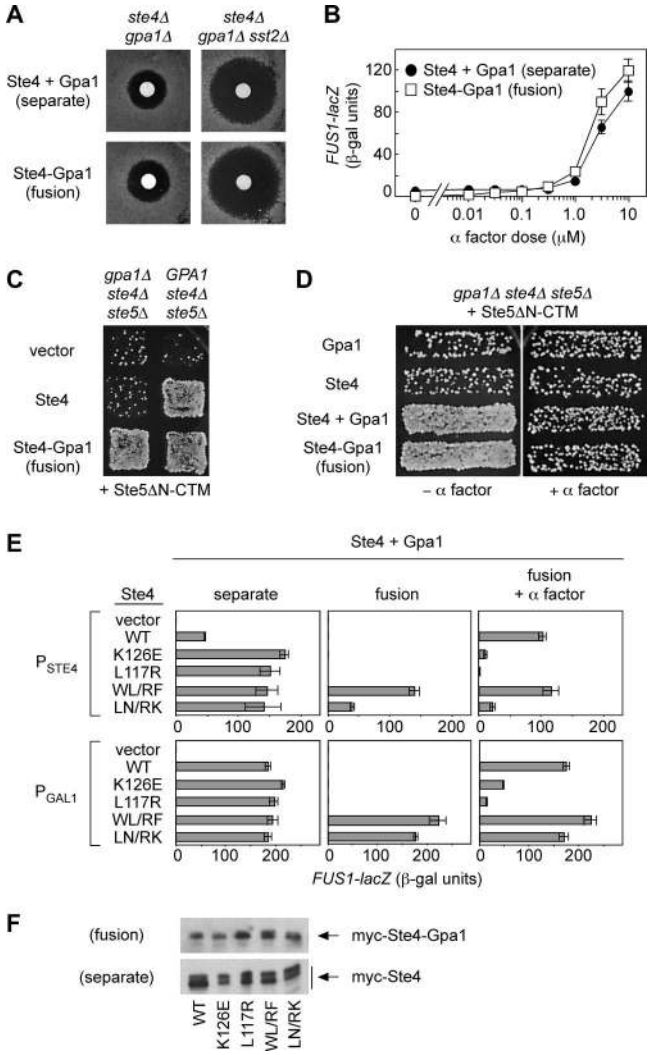

Figure 7. Phenotypes of Ste4–Gpa1 fusion proteins. (A) A Ste4–Gpa1 fusion expressed from the native *STE4* promoter functions indistinguishably from separate Ste4 and Gpa1 polypeptides. Halo assays show growth arrest of *ste4*Δ *gpa1*Δ cells (PPY1228) or *ste4*Δ *gpa1*Δ *sst2*Δ cells (PPY1942) harboring Gpa1 and Ste4 as separate (YCplac22-GPA1-WT + pPP226) or fused (pPP1340 + pRS314 vector) polypeptides. (B) *FUS1-lacZ* assays (mean ± SD; n = 4) showing that the Ste4-Gpa1 fusion retains a normal dose response to pheromone. PPY1663 (*ste4*Δ *gpa1*Δ) harbored plasmids as in A. Cells were treated with the indicated concentration of α factor for 2 h. (C) Patch mating assay of strains PPY1230 (*ste5*Δ *ste4*Δ *gpa1*Δ*)* or PPY886 (*ste5*Δ *ste4*Δ *GPA1*) harboring P_{GAL1}-*STE5*Δ*N-CTM* (pPP473) plus pRS316, pPP226, or pPP1340. (D) Patch mating assays showing that the Ste4-Gpa1 fusion protein remains proficient at chemotropism. Strain PPY1230 carried P_{GAL1}-*STE5*Δ*N-CTM* (pPP479) and the following plasmid combinations: pPP2711 + pRS316, pRS314 + pPP226, pPP2711 + pPP226, or pRS314 + pPP1340. (E) The Ste4-Gpa1 fusion context reveals distinct signaling phenotypes for the Ste4 Nt and Sw mutants. Top, strain PPY1662 (*ste4*Δ *ste7*Δ) harbored a P_{GAL1}-*STE7* construct (pPP2773) plus either vector (pRS316) or the indicated *STE4* or *STE4-GPA1* fusion alleles, expressed from the native *STE4* promoter. Bottom, strain PPY856 (*ste4*Δ) harbored either vector (pPP446) or the indicated P_{GAL1}-*STE4* or P_{GAL1}-*STE4-GPA1* fusion constructs. *FUS1-lacZ* activation was measured after induction with galactose ± α factor. Bars, mean ± SD (n = 4). (F) The Ste4 mutations do not affect protein levels. Lysates of cells harboring myc-tagged Ste4 (derivatives of pPP2838) or myc-tagged Ste4-Gpa1 (derivatives of pPP2839) were analyzed by anti-myc immunoblot. (Relevant portions of each blot are shown; as expected, myc-Ste4-Gpa1 runs considerably larger than myc-Ste4.)

was detrimental, because cells expressing Gpa1-QL could not polarize even after exposure to pheromone (Figure 8, A and B, + α factor). Therefore, polarization requires more than just the acquisition of both GTP-bound Gα and active Gβγ.

It seemed possible that activated Gα and Gβγ subunits might have to remain in close mutual proximity and that this might be accomplished during receptor-mediated activation but not by coexpression of mutationally activated subunits. Therefore, to force GTP-bound Gα to remain associated with Gβγ, we incorporated the Gpa1-QL mutation into the Ste4–Gpa1 fusion. In signaling assays, either the Ste4-WL/RF or Gpa1-QL mutations (or both) caused constitutive activity (Figure 8C); yet, none of these fusions could induce de novo polarization in the absence of pheromone (Figure 8, A and B, −α factor). Notably, the fusions containing the Gpa1-QL mutation did promote a detectable increase in elongation (and more so than when the same subunits were expressed as separate polypeptides), but these elongated cells did not form the pointed, pear-shaped shmoos seen during pheromone treatment. Thus, the cells were still missing some aspect of pheromone-induced polarization that can focus morphogenesis to a restricted portion of the cell perimeter.

Furthermore, the ability of pheromone to trigger de novo polarization remained intact when Ste4 was fused to Gpa1, but this was disrupted by the Gpa1-QL mutation (Figure 8, A and B, +α factor). Consistent with these findings, the fusions containing the Gpa1-QL mutation were also defective in chemotropic mating assays (Figure 8D), and the Gpa1-QL mutant (expressed as a separate polypeptide) eliminated the mating advantage of Sw interface mutants over Nt interface mutants (Figure 8E). Thus, interfering with GTP hydrolysis activates Gβγ signaling, but it disrupts cell polarization and chemotropism, regardless of whether Gα is fused to Gβ or kept separate. Finally, it should be noted that the chemotropism and polarity defects shown by the Gpa1-QL mutant are recessive to wild-type Gpa1 (unpublished observations). Together, these findings suggest that the ability of pheromone-bound receptor molecules to guide cell polarization, either along a de novo polarization axis or along pheromone gradients, requires normal coupling to the Gα GTP hydrolysis cycle.

DISCUSSION

This work examines how a GPCR and its coupled Gαβγ heterotrimer coordinate an asymmetric response to external stimuli. Our findings indicate that although yeast Gβγ is known to interact with downstream polarity factors (e.g., Far1, Cdc24), proper control of cell polarity in either the presence or absence of pheromone gradients requires an intact receptor-Gαβγ module and a normal GTP–GDP cycle on Gα. Furthermore, our results suggest distinct roles for the two Gα–Gβ interaction interfaces, whereby the Sw interface controls signaling and the Nt interface governs coupling to the receptor. As such, pheromone control of polarity requires maintenance of the Nt interface but not the Sw interface. Overall, these results suggest that continuous communication between the receptor and Gαβγ is important for chemotropism and polarized growth, perhaps to regulate Gαβγ in a spatially asymmetric manner.

Distinctions between Signaling and Polarity Roles of Gβγ

Bypassing the role of Gβγ in signaling revealed several interesting points regarding mating and cell polarization. First, the ability of pheromone and Gβγ to regulate chemot-

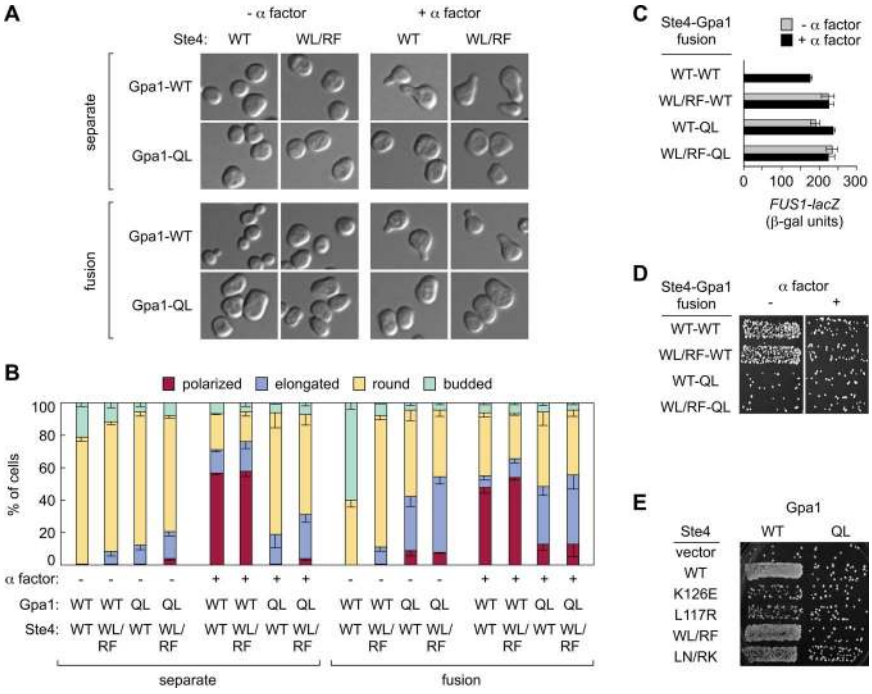

Figure 8. Polarity control requires GTP hydrolysis by Gpa1. (A and B) De novo polarization was monitored using *ste4*Δ *gpa1*Δ *rsr1*Δ cells (PPY1380) expressing Ste4 and Gpa1 variants as either separate or fused polypeptides, after 4-h induction with galactose ± α factor. Separate Ste4 and Gpa1 subunits were expressed from pPP1151, pPP1228 (= WL/RF derivative of pPP1151), pPP2711, and pPP2802. Ste4–Gpa1 fusions were expressed from derivatives of pPP1150. The Gpa1-QL mutant is defective at GTP hydrolysis. (A) Representative images of the predominant morphologies. (B) Cell morphologies were quantified by blind counting of 200 cells per condition in three separate experiments. Cells were scored as "polarized" if they formed pear-shaped shmoos or elongated to a point at one end; cells were scored as "elongated" if one axis was clearly longer than the other but neither end was pointed. Bars, mean − SD (n = 3). (C) Transcriptional induction. PPY856 (*ste4*Δ) cells harboring the indicated P_{GAL1}-*STE4-GPA1* plasmids (derivatives of pPP1150) were induced with galactose ± α factor. Results for the WT–WT and WL/RF–WT fusion proteins are identical to those for the P_{GAL1}-driven constructs in Figure 7E (bottom, middle and right), and they are shown here for comparison. Bars, mean ± SD (n = 4). (D) Fusion proteins harboring the Gpa1-QL mutation are defective at chemotropism. Mating was assayed ± 20 μM α factor by using strain PPY1230 (*ste4*Δ *gpa1*Δ *ste5*Δ) expressing P_{GAL1}-*STE5*Δ*N-CTM* (pPP479) and Ste4-Gpa1 fusions (as in C). (E) Gpa1-QL eliminates the chemotropic advantage of Sw interface mutants over Nt interface mutants. Mating was assayed in strain PPY1230 (*ste4*Δ *gpa1*Δ *ste5*Δ) expressing P_{GAL1}-*STE5*Δ*N-SEC22* (pPP1175) and the indicated combination of Gpa1 (pPP2711, pPP2802) and Ste4 (derivatives of pPP226; vector = pRS316).

ropism or de novo polarization does not require the ability to modulate MAP kinase cascade signaling or the presence of the scaffold protein Ste5 (see Figures 1 and 2). Second, the level of mating success is neither solely dictated by nor strongly dependent on transcription levels, because the two membrane-targeted Ste5 reagents activated transcription to either high (Ste5ΔN-CTM) or low (Ste5ΔN-Sec22) levels and yet yielded higher efficiency mating than the Ste11 and Ste12 reagents (Figure 1). Presumably, the Ste5 reagents promote the most efficient mating because they can activate the MAP kinase cascade (i.e., in contrast to Ste12 overexpression, which induces transcription only), but they do not cross-activate other pathways that inhibit mating (i.e., in contrast to Ste11ΔN, which also activates the HOG pathway) (Harris *et al*., 2001). Third, the ability of pheromone gradients to increase mating success is independent of the baseline level of mating, as this behavior was observed whether the baseline level of mating was relatively high (Ste5ΔN-CTM and Ste5ΔN-Sec22) or relatively low (Ste11ΔN and Ste12) (Figure 1).

Heterotrimeric G Protein Dissociation

Several of our findings are relevant to the mechanism of Gαβγ dissociation. Although it is generally accepted that nucleotide exchange causes Gα-GTP to dissociate from Gβγ (Gilman, 1987; Neer, 1995; Cabrera-Vera *et al*., 2003), some studies suggest that complete dissociation may not be necessary (Rebois *et al*., 1997; Klein *et al*., 2000; Levitzki and Klein, 2002; Bunemann *et al*., 2003; Gales *et al*., 2006). Indeed, prior work showed that the yeast heterotrimer remained functional when Gα and Gβ were expressed as a Gβ–Gα fusion protein (Klein *et al*., 2000), which should restrict dissociation. We extended these results by showing that this Gβ–Gα fusion protein performs both signaling and polarity functions indistinguishably from the wild-type (unfused) proteins, even when expressed at native levels. Moreover, the chemotropic and de novo polarization proficiency we observed with the Sw interface mutants indicates that despite being active for signaling, they can still mediate a response to the pheromone ligand whereas the Nt interface mutants cannot. This implies that the Sw mutants maintain a functional Nt interface and hence raises the possibility that the Gαβγ heterotrimer may remain tethered by the Nt interface, allowing continued communication with the receptor (Figure 9). By extension, it is conceivable that this "partial dissociation" state applies not only to the Sw interface mutants but also to receptor-activated Gαβγ. That is, GTP-induced conformational changes in the Switch region of Gα may trigger an initial state in which the Sw interface dissociates but the Nt interface does not.

Several structural considerations are pertinent to this partial dissociation model. First, the N-terminal helix of Gα is implicated in receptor recognition, and it is thought to lie tangential to the membrane (Taylor *et al*., 1994; Bourne, 1997; Hamm, 1998, 2001; Itoh *et al*., 2001; Cabrera-Vera *et al*., 2003). Second, Gαβγ is anchored to the membrane by addition of lipophilic groups to the Gα N terminus and the Gγ C terminus (Wedegaertner *et al*., 1995), which lie adjacent to each other at one end of the Nt interface (Wall *et al*., 1995; Lambright *et al*., 1996) (Figure 9). Membrane insertion of these groups stabilizes the intact heterotrimer (Bigay *et al*., 1994); thus, it may also stabilize the weak interaction at the Nt interface enough to keep the partially dissociated structure intact in vivo but not in detergent-solubilized cell extracts. Third, the behavior of the Gβ–Gα fusion protein is compatible with the partial dissociation model, because the link formed between the Gβ C terminus and the Gα N terminus would constrain separation of the Nt interface but not the

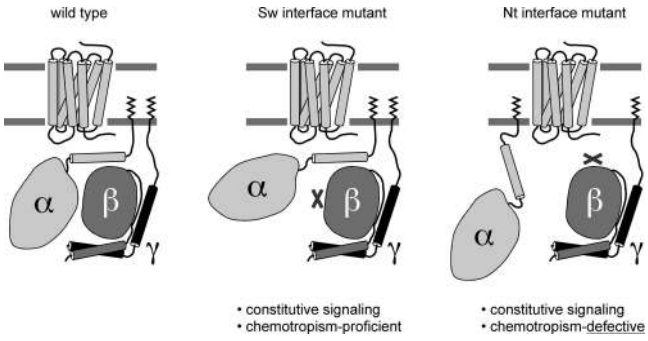

Figure 9. Model for how Sw and Nt mutants differentially affect dissociation of G$\alpha\beta\gamma$ and receptor coupling. The schematic diagram of the receptor and heterotrimer is based on the molecular model shown in Figure 3A. Zig-zag lines signify membrane-anchoring groups attached to the N terminus of Gα and the C terminus of Gγ. Mutations in either the Sw or Nt interface cause constitutive activation of G$\beta\gamma$, but the Sw interface mutants remain competent to mediate directional responses to chemoattractant (i.e., chemotropism and de novo polarization), whereas the Nt interface mutants are defective. Alone, contacts in the Nt interface may be insufficient to maintain Gα–Gβ association, but membrane insertion of the adjacent lipophilic groups may stabilize this weak interaction; this could explain why the Sw interface mutants show no Gα interaction in the absence of membranes (e.g., in coimmunoprecipitation and two-hybrid assays), and yet can still mediate responses to pheromone in vivo. Therefore, mutations in the Sw interface are proposed to result in a partially dissociated structure that remains tethered by the Nt interface, and hence remains in regulatory communication with the receptor. See text for further discussion.

Sw interface. Fourth, crystal structures of G$\alpha\beta\gamma$ show that the N-terminal helix of Gα makes no tertiary contacts with the remainder of Gα (Wall *et al*., 1995; Lambright *et al*., 1996), and so the intervening linkage could freely rotate to allow the Gα and Gβ halves of the Sw interface to swivel apart. Cocrystal structures are also compatible with partial dissociation, because contacts between G$\beta\gamma$ and effectors involve residues in the Sw interface rather than the Nt interface (Gaudet *et al*., 1996; Lodowski *et al*., 2003).

Note that this partial dissociation model does not postulate that Gα and G$\beta\gamma$ are inseparable, but only that dissociation of the Sw interface does not automatically lead to dissociation of the Nt interface as a necessary or immediate consequence. Complete dissociation might follow if GTP hydrolysis is slow or when Gα-GTP and G$\beta\gamma$ bind their targets (Tesmer *et al*., 2005). Partial dissociation could be advantageous by allowing an additional level of heterotrimer regulation or by accelerating heterotrimer reformation after GTP hydrolysis by Gα. In our physiological context, it could facilitate chemotropism and de novo polarization by allowing activated G$\beta\gamma$ to remain in regulatory communication with the receptor.

Symmetry Breaking and De Novo Polarization

Symmetry breaking, in which cells or molecular modules self-polarize without a localized cue, is thought to involve the amplification of an initial asymmetry that occurs through stochastic variation (Kirschner *et al*., 2000; Wedlich-Soldner and Li, 2003). In yeast, symmetry breaking can produce polarized buds in the absence of directional cues (Chant and Herskowitz, 1991; Irazoqui *et al*., 2003). This has been proposed to result from stochastic variation in the local amount of activated (GTP-bound) Cdc42, which is then amplified by positive feedback loops via two possible pathways. One pathway involves self-assembly of the adaptor protein Bem1, which links Cdc24 and Cdc42 (Butty *et al*., 2002; Irazoqui *et al*., 2003; Wedlich-Soldner *et al*., 2004). The other pathway involves feedback between Cdc42-induced actin polymerization and polarized transport of secretory vesicles carrying Cdc42 as cargo (Gulli *et al*., 2000; Wedlich-Soldner *et al*., 2003; Wedlich-Soldner and Li, 2003).

Analogous mechanisms may apply during pheromone response to allow de novo polarization. In principle, breaking the symmetry inherent in a uniform field of pheromone could begin with small differences in receptor–G$\alpha\beta\gamma$ activation. However, our results indicate that activation of the MAP kinase cascade is sufficient to trigger some asymmetry even in the absence of pheromone or G protein subunits. Furthermore, previous studies show that establishment and maintenance of the polarity axis are separable (Nern and Arkowitz, 2000) and that the MAP kinase Fus3 is required to establish asymmetry (Matheos *et al*., 2004). Hence, the most parsimonious model may be that the MAP kinase pathway imparts the polarity machinery with some inherent self-organizational ability, whereas the receptor–G$\alpha\beta\gamma$ module controls orientation and directional persistence, either by influencing the initial directional choice or by providing continuous reinforcement of the initial asymmetry.

Our findings implicate a role for continuous communication between pheromone-bound receptors and G$\alpha\beta\gamma$, because activated G$\beta\gamma$ and Gα alone cannot promote directionally persistent polarization. Because pheromone receptors are rapidly internalized and redelivered by secretory transport along actin filaments (Jenness and Spatrick, 1986; Schandel and Jenness, 1994; Ayscough and Drubin, 1998), initial asymmetries might become amplified by polarized delivery of new pheromone receptors to the initial landmark, resulting in heightened pheromone response in that location which would reinforce the initial directional choice. The mutations that disrupt de novo polarization (i.e., *gpa1-Q323L*, or *ste4* Nt interface mutations) may disable this positive reinforcement by disrupting the ability to coordinate receptor localization with the activity/localization of Gα, G$\beta\gamma$, or both. In contrast, the behavior of the Sw interface mutants suggests that, despite constitutively active G$\beta\gamma$ signaling, these mutant heterotrimers remain in regulatory communication with the receptor. Although it remains unclear what this communication achieves in molecular terms, we envision three speculative scenarios: 1) interaction with asymmetrically localized receptors might influence localization of the heterotrimer, thereby causing asymmetrically localized G$\beta\gamma$ activity; 2) the Sw mutants might allow nucleotide exchange on the Gα subunit at sites of pheromone-bound receptors, potentially promoting localized Gα-GTP, which could control polarization in synergy with G$\beta\gamma$; or 3) pheromone-bound receptors might interact directly with downstream polarity factors, but normal affinity of receptors for ligand might require coupling to a G$\alpha\beta\gamma$ heterotrimer with an intact Nt interface and normal GDP-GTP exchange properties. Distinguishing among these scenarios will require further study.

GTP Hydrolysis and Localized Signaling

GTP hydrolysis is important for polarity control by Cdc42 in both yeast and mammalian cells (Stowers *et al*., 1995; Irazoqui *et al*., 2003). Similarly, we found that chemotropism and de novo polarization require GTP hydrolysis by the Gα subunit Gpa1. To provide a directional cue, GTP loading of Gα and the resultant activation of G$\beta\gamma$ may have to occur in a localized manner, which would be obscured if all Gα molecules were locked in the GTP-bound state and distrib-

uted uniformly. Thus, the spatial distribution of active signaling molecules is likely to be critical to their function in guiding cell polarity. To focus this spatial distribution, the activities of these proteins may also need to be rapidly extinguished by mechanisms such as by GTP hydrolysis, phosphorylation, or endocytosis. Indeed, chemotaxis is thought to depend on a combination of local excitation and global inhibition of polarization activities (Iijima *et al*., 2002). Endocytic clearing allows directionally transported membrane proteins to maintain a polarized distribution (Valdez-Taubas and Pelham, 2003; Marco *et al*., 2007), and pheromone-regulated polarization in yeast is facilitated by endocytosis signals in receptor C termini (Konopka *et al*., 1988; Vallier *et al*., 2002). Thus, localized signaling and delivery may generally work in concert with down-regulatory mechanisms to ensure proper polarity control.

CONCLUSIONS

The findings reported here reveal several unexpected lessons that may be applicable to other examples of cell polarity control, heterotrimeric G protein function, or both. First, the activated Gαβγ heterotrimer (and the resulting downstream signaling) is not inherently able to organize a directionally persistent polarization axis. Second, the requirements of the receptor–Gαβγ module are similar for gradient-controlled polarization and de novo polarization. Third, the two structurally distinct Gα–Gβ interfaces have functionally distinct roles. Fourth, the yeast heterotrimer may be able to function in a partially dissociated state that allows continued regulatory communication with the receptor. In future studies, it will be interesting to compare these behaviors shown by the yeast system to those of other systems.

ACKNOWLEDGMENTS

We thank Henrik Dohlman, Alexander Levitzki, David Stone, and Malcolm Whiteway for plasmids, as well as thank Danny Lew and Dan McCollum for comments on the manuscript. We are especially indebted to Rachel Lamson and Matt Winters for technical assistance during the completion and revision stages. This work was supported by a grant from the National Institutes of Health (GM57769) to P.M.P.

REFERENCES

Apanovitch, D. M., Iiri, T., Karasawa, T., Bourne, H. R., and Dohlman, H. G. (1998). Second site suppressor mutations of a GTPase-deficient G-protein α-subunit. Selective inhibition of Gβγ-mediated signaling. J. Biol. Chem. *273*, 28597–28602.

Arkowitz, R. A. (1999). Responding to attraction: chemotaxis and chemotropism in *Dictyostelium* and yeast. Trends Cell Biol. *9*, 20–27.

Ayscough, K. R., and Drubin, D. G. (1998). A role for the yeast actin cytoskeleton in pheromone receptor clustering and signalling. Curr. Biol. *8*, 927–930.

Bagorda, A., Mihaylov, V. A., and Parent, C. A. (2006). Chemotaxis: moving forward and holding on to the past. Thromb. Haemost. *95*, 12–21.

Bar, E. E., Ellicott, A. T., and Stone, D. E. (2003). Gbetagamma recruits Rho1 to the site of polarized growth during mating in budding yeast. J. Biol. Chem. *278*, 21798–21804.

Bartel, P. L., and Fields, S. (1995). Analyzing protein-protein interactions using two-hybrid system. Methods Enzymol. *254*, 241–263.

Bigay, J., Faurobert, E., Franco, M., and Chabre, M. (1994). Roles of lipid modifications of transducin subunits in their GDP-dependent association and membrane binding. Biochemistry *33*, 14081–14090.

Bourne, H. R. (1997). How receptors talk to trimeric G proteins. Curr. Opin. Cell Biol. *9*, 134–142.

Bunemann, M., Frank, M., and Lohse, M. J. (2003). Gi protein activation in intact cells involves subunit rearrangement rather than dissociation. Proc. Natl. Acad. Sci. USA *100*, 16077–16082.

Butty, A. C., Perrinjaquet, N., Petit, A., Jaquenoud, M., Segall, J. E., Hofmann, K., Zwahlen, C., and Peter, M. (2002). A positive feedback loop stabilizes the guanine-nucleotide exchange factor Cdc24 at sites of polarization. EMBO J. *21*, 1565–1576.

Butty, A. C., Pryciak, P. M., Huang, L. S., Herskowitz, I., and Peter, M. (1998). The role of Far1p in linking the heterotrimeric G protein to polarity establishment proteins during yeast mating. Science *282*, 1511–1516.

Cabrera-Vera, T. M., Vanhauwe, J., Thomas, T. O., Medkova, M., Preininger, A., Mazzoni, M. R., and Hamm, H. E. (2003). Insights into G protein structure, function, and regulation. Endocr. Rev. *24*, 765–781.

Cairns, B. R., Ramer, S. W., and Kornberg, R. D. (1992). Order of action of components in the yeast pheromone response pathway revealed with a dominant allele of the STE11 kinase and the multiple phosphorylation of the STE7 kinase. Genes Dev. *6*, 1305–1318.

Chant, J. (1999). Cell polarity in yeast. Annu. Rev. Cell Dev. Biol. *15*, 365–391.

Chant, J., and Herskowitz, I. (1991). Genetic control of bud site selection in yeast by a set of gene products that constitute a morphogenetic pathway. Cell *65*, 1203–1212.

Dohlman, H. G., Song, J., Ma, D., Courchesne, W. E., and Thorner, J. (1996). Sst2, a negative regulator of pheromone signaling in the yeast *Saccharomyces cerevisiae*: expression, localization, and genetic interaction and physical association with Gpa1 (the G-protein α subunit). Mol. Cell Biol. *16*, 5194–5209.

Dohlman, H. G., and Thorner, J. W. (2001). Regulation of G protein-initiated signal transduction in yeast: paradigms and principles. Annu. Rev. Biochem. *70*, 703–754.

Dolan, J. W., and Fields, S. (1990). Overproduction of the yeast STE12 protein leads to constitutive transcriptional induction. Genes Dev. *4*, 492–502.

Dorer, R., Pryciak, P. M., and Hartwell, L. H. (1995). Saccharomyces cerevisiae cells execute a default pathway to select a mate in the absence of pheromone gradients. J. Cell Biol. *131*, 845–861.

Dowell, S. J., Bishop, A. L., Dyos, S. L., Brown, A. J., and Whiteway, M. S. (1998). Mapping of a yeast G protein betagamma signaling interaction. Genetics *150*, 1407–1417.

Etienne-Manneville, S. (2004). Cdc42–the centre of polarity. J. Cell Sci. *117*, 1291–1300.

Feng, Y., Song, L. Y., Kincaid, E., Mahanty, S. K., and Elion, E. A. (1998). Functional binding between Gβ and the LIM domain of Ste5 is required to activate the MEKK Ste11. Curr. Biol. *8*, 267–278.

Franca-Koh, J., Kamimura, Y., and Devreotes, P. (2006). Navigating signaling networks: chemotaxis in *Dictyostelium discoideum*. Curr. Opin. Genet Dev. *16*, 333–338.

Gales, C., Van Durm, J. J., Schaak, S., Pontier, S., Percherancier, Y., Audet, M., Paris, H., and Bouvier, M. (2006). Probing the activation-promoted structural rearrangements in preassembled receptor-G protein complexes. Nat. Struct. Mol. Biol. *13*, 778–786.

Gartner, A., Jovanovic, A., Jeoung, D. I., Bourlat, S., Cross, F. R., and Ammerer, G. (1998). Pheromone-dependent G1 cell cycle arrest requires Far1 phosphorylation, but may not involve inhibition of Cdc28-Cln2 kinase, in vivo. Mol. Cell Biol. *18*, 3681–3691.

Gaudet, R., Bohm, A., and Sigler, P. B. (1996). Crystal structure at 2.4 Å resolution of the complex of transducin βγ and its regulator, phosducin. Cell *87*, 577–588.

Gilman, A. G. (1987). G proteins: transducers of receptor-generated signals. Annu. Rev. Biochem. *56*, 615–649.

Grishin, A. V., Weiner, J. L., and Blumer, K. J. (1994a). Biochemical and genetic analysis of dominant-negative mutations affecting a yeast G-protein γ subunit. Mol. Cell Biol. *14*, 4571–4578.

Grishin, A. V., Weiner, J. L., and Blumer, K. J. (1994b). Control of adaptation to mating pheromone by G protein β subunits of *Saccharomyces cerevisiae*. Genetics *138*, 1081–1092.

Gulli, M., Jaquenoud, M., Shimada, Y., Niederhauser, G., Wiget, P., and Peter, M. (2000). Phosphorylation of the Cdc42 exchange factor Cdc24 by the PAK-like kinase Cla4 may regulate polarized growth in yeast. Mol. Cell *6*, 1155–1167.

Hamm, H. E. (1998). The many faces of G protein signaling. J. Biol. Chem. *273*, 669–672.

Hamm, H. E. (2001). How activated receptors couple to G proteins. Proc. Natl. Acad. Sci. USA *98*, 4819–4821.

Harris, K., Lamson, R. E., Nelson, B., Hughes, T. R., Marton, M. J., Roberts, C. J., Boone, C., and Pryciak, P. M. (2001). Role of scaffolds in MAP kinase pathway specificity revealed by custom design of pathway-dedicated signaling proteins. Curr. Biol. *11*, 1815–1824.

Hollenberg, S. M., Sternglanz, R., Cheng, P. F., and Weintraub, H. (1995). Identification of a new family of tissue-specific basic helix-loop-helix proteins with a two-hybrid system. Mol. Cell Biol. *15*, 3813–3822.

Iijima, M., Huang, Y. E., and Devreotes, P. (2002). Temporal and spatial regulation of chemotaxis. Dev. Cell *3*, 469–478.

Inouye, C., Dhillon, N., and Thorner, J. (1997). Ste5 RING-H2 domain: role in Ste4-promoted oligomerization for yeast pheromone signaling. Science *278*, 103–106.

Irazoqui, J. E., Gladfelter, A. S., and Lew, D. J. (2003). Scaffold-mediated symmetry breaking by Cdc42p. Nat. Cell Biol. *5*, 1062–1070.

Itoh, Y., Cai, K., and Khorana, H. G. (2001). Mapping of contact sites in complex formation between light-activated rhodopsin and transducin by covalent crosslinking: use of a chemically preactivated reagent. Proc. Natl. Acad. Sci. USA *98*, 4883–4887.

Jackson, C. L., and Hartwell, L. H. (1990). Courtship in *S. cerevisiae*: both cell types choose mating partners by responding to the strongest pheromone signal. Cell *63*, 1039–1051.

Jackson, C. L., Konopka, J. B., and Hartwell, L. H. (1991). *S. cerevisiae* α pheromone receptors activate a novel signal transduction pathway for mating partner discrimination. Cell *67*, 389–402.

Jenness, D. D., and Spatrick, P. (1986). Down regulation of the α-factor pheromone receptor in *S. cerevisiae*. Cell *46*, 345–353.

Kirschner, M., Gerhart, J., and Mitchison, T. (2000). Molecular "vitalism." Cell *100*, 79–88.

Klein, S., Reuveni, H., and Levitzki, A. (2000). Signal transduction by a nondissociable heterotrimeric yeast G protein. Proc. Natl. Acad. Sci. USA *97*, 3219–3223.

Konopka, J. B., Jenness, D. D., and Hartwell, L. H. (1988). The C-terminus of the *S. cerevisiae* alpha-pheromone receptor mediates an adaptive response to pheromone. Cell *54*, 609–620.

Lambright, D. G., Sondek, J., Bohm, A., Skiba, N. P., Hamm, H. E., and Sigler, P. B. (1996). The 2.0 Å crystal structure of a heterotrimeric G protein. Nature *379*, 311–319.

Lamson, R. E., Winters, M. J., and Pryciak, P. M. (2002). Cdc42 regulation of kinase activity and signaling by the yeast p21-activated kinase Ste20. Mol. Cell Biol. *22*, 2939–2951.

Leberer, E., Dignard, D., Harcus, D., Thomas, D. Y., and Whiteway, M. (1992). The protein kinase homologue Ste20p is required to link the yeast pheromone response G-protein $\beta\gamma$ subunits to downstream signalling components. EMBO J. *11*, 4815–4824.

Leeuw, T., Wu, C., Schrag, J. D., Whiteway, M., Thomas, D. Y., and Leberer, E. (1998). Interaction of a G-protein β-subunit with a conserved sequence in Ste20/PAK family protein kinases. Nature *391*, 191–195.

Levitzki, A., and Klein, S. (2002). G-protein subunit dissociation is not an integral part of G-protein action. Chembiochemistry *3*, 815–818.

Lodowski, D. T., Pitcher, J. A., Capel, W. D., Lefkowitz, R. J., and Tesmer, J. J. (2003). Keeping G proteins at bay: a complex between G protein-coupled receptor kinase 2 and G$\beta\gamma$. Science *300*, 1256–1262.

Madden, K., and Snyder, M. (1992). Specification of sites for polarized growth in *Saccharomyces cerevisiae* and the influence of external factors on site selection. Mol. Biol. Cell *3*, 1025–1035.

Mahanty, S. K., Wang, Y., Farley, F. W., and Elion, E. A. (1999). Nuclear shuttling of yeast scaffold Ste5 is required for its recruitment to the plasma membrane and activation of the mating MAPK cascade. Cell *98*, 501–512.

Marco, E., Wedlich-Soldner, R., Li, R., Altschuler, S. J., and Wu, L. F. (2007). Endocytosis optimizes the dynamic localization of membrane proteins that regulate cortical polarity. Cell *129*, 411–422.

Matheos, D., Metodiev, M., Muller, E., Stone, D., and Rose, M. D. (2004). Pheromone-induced polarization is dependent on the Fus3p MAPK acting through the formin Bni1p. J. Cell Biol. *165*, 99–109.

Metodiev, M. V., Matheos, D., Rose, M. D., and Stone, D. E. (2002). Regulation of MAPK function by direct interaction with the mating-specific Gα in yeast. Science *296*, 1483–1486.

Moskow, J. J., Gladfelter, A. S., Lamson, R. E., Pryciak, P. M., and Lew, D. J. (2000). Role of Cdc42p in pheromone-stimulated signal transduction in *Saccharomyces cerevisiae*. Mol. Cell Biol. *20*, 7559–7571.

Neer, E. J. (1995). Heterotrimeric G proteins: organizers of transmembrane signals. Cell *80*, 249–257.

Neiman, A. M., and Herskowitz, I. (1994). Reconstitution of a yeast protein kinase cascade in vitro: activation of the yeast MEK homologue STE7 by STE11. Proc. Natl. Acad. Sci. USA *91*, 3398–3402.

Nern, A., and Arkowitz, R. A. (1998). A GTP-exchange factor required for cell orientation. Nature *391*, 195–198.

Nern, A., and Arkowitz, R. A. (1999). A Cdc24p-Far1p-G$\beta\gamma$ protein complex required for yeast orientation during mating. J. Cell Biol. *144*, 1187–1202.

Nern, A., and Arkowitz, R. A. (2000). G proteins mediate changes in cell shape by stabilizing the axis of polarity. Mol. Cell *5*, 853–864.

Pruyne, D., and Bretscher, A. (2000). Polarization of cell growth in yeast. I. Establishment and maintenance of polarity states. J. Cell Sci. *113*, 365–375.

Pryciak, P. M., and Hartwell, L. H. (1996). AKR1 encodes a candidate effector of the G$\beta\gamma$ complex in the *Saccharomyces cerevisiae* pheromone response pathway and contributes to control of both cell shape and signal transduction. Mol. Cell Biol. *16*, 2614–2626.

Pryciak, P. M., and Huntress, F. A. (1998). Membrane recruitment of the kinase cascade scaffold protein Ste5 by the G$\beta\gamma$ complex underlies activation of the yeast pheromone response pathway. Genes Dev. *12*, 2684–2697.

Rebois, R. V., Warner, D. R., and Basi, N. S. (1997). Does subunit dissociation necessarily accompany the activation of all heterotrimeric G proteins? Cell Signal *9*, 141–151.

Roberts, C. J. *et al*. (2000). Signaling and circuitry of multiple MAPK pathways revealed by a matrix of global gene expression profiles. Science *287*, 873–880.

Schandel, K. A., and Jenness, D. D. (1994). Direct evidence for ligand-induced internalization of the yeast α-factor pheromone receptor. Mol. Cell Biol. *14*, 7245–7255.

Schrick, K., Garvik, B., and Hartwell, L. H. (1997). Mating in *Saccharomyces cerevisiae*: the role of the pheromone signal transduction pathway in the chemotropic response to pheromone. Genetics *147*, 19–32.

Segall, J. E. (1993). Polarization of yeast cells in spatial gradients of α mating factor. Proc. Natl. Acad. Sci. USA *90*, 8332–8336.

Sikorski, R. S., and Hieter, P. (1989). A system of shuttle vectors and yeast host strains designed for efficient manipulation of DNA in *Saccharomyces cerevisiae*. Genetics *122*, 19–27.

Sohrmann, M., and Peter, M. (2003). Polarizing without a c(l)ue. Trends Cell Biol. *13*, 526–533.

Sondek, J., Bohm, A., Lambright, D. G., Hamm, H. E., and Sigler, P. B. (1996). Crystal structure of a G_A protein $\beta\gamma$ dimer at 2.1 Å resolution. Nature *379*, 369–374.

Stone, D. E., and Reed, S. I. (1990). G protein mutations that alter the pheromone response in *Saccharomyces cerevisiae*. Mol. Cell Biol. *10*, 4439–4446.

Stowers, L., Yelon, D., Berg, L. J., and Chant, J. (1995). Regulation of the polarization of T cells toward antigen-presenting cells by Ras-related GTPase CDC42. Proc. Natl. Acad. Sci. USA *92*, 5027–5031.

Stratton, H. F., Zhou, J., Reed, S. I., and Stone, D. E. (1996). The mating-specific Gα protein of *Saccharomyces cerevisiae* downregulates the mating signal by a mechanism that is dependent on pheromone and independent of G$\beta\gamma$ sequestration. Mol. Cell. Biol. *16*, 6325–6337.

Strickfaden, S. C., Winters, M. J., Ben-Ari, G., Lamson, R. E., Tyers, M., and Pryciak, P. M. (2007). A Mechanism for cell-cycle regulation of MAP kinase signaling in a yeast differentiation pathway. Cell *128*, 519–531.

Taylor, J. M., Jacob-Mosier, G. G., Lawton, R. G., Remmers, A. E., and Neubig, R. R. (1994). Binding of an α_2 adrenergic receptor third intracellular loop peptide to Gβ and the amino terminus of Gα. J. Biol. Chem. *269*, 27618–27624.

Tesmer, V. M., Kawano, T., Shankaranarayanan, A., Kozasa, T., and Tesmer, J. J. (2005). Snapshot of activated G proteins at the membrane: the $G\alpha_q$-GRK2-G$\beta\gamma$ complex. Science *310*, 1686–1690.

Valdez-Taubas, J., and Pelham, H. R. (2003). Slow diffusion of proteins in the yeast plasma membrane allows polarity to be maintained by endocytic cycling. Curr. Biol. *13*, 1636–1640.

Vallier, L. G., Segall, J. E., and Snyder, M. (2002). The alpha-factor receptor C-terminus is important for mating projection formation and orientation in *Saccharomyces cerevisiae*. Cell Motil. Cytoskeleton *53*, 251–266.

Valtz, N., Peter, M., and Herskowitz, I. (1995). FAR1 is required for oriented polarization of yeast cells in response to mating pheromones. J. Cell Biol. *131*, 863–873.

van Drogen, F., O'Rourke, S. M., Stucke, V. M., Jaquenoud, M., Neiman, A. M., and Peter, M. (2000). Phosphorylation of the MEKK Ste11p by the

PAK-like kinase Ste20p is required for MAP kinase signaling in vivo. Curr. Biol. *10*, 630–639.

van Drogen, F., Stucke, V. M., Jorritsma, G., and Peter, M. (2001). MAP kinase dynamics in response to pheromones in budding yeast. Nat. Cell Biol. *3*, 1051–1059.

Wall, M. A., Coleman, D. E., Lee, E., Iñiguez-Lluhi, J. A., Posner, B. A., Gilman, A. G., and Sprang, S. R. (1995). The structure of the G protein heterotrimer $G_{i\alpha1}\beta_1\gamma_2$. Cell *83*, 1047–1058.

Wedegaertner, P. B., Wilson, P. T., and Bourne, H. R. (1995). Lipid modifications of trimeric G proteins. J. Biol. Chem. *270*, 503–506.

Wedlich-Soldner, R., Altschuler, S., Wu, L., and Li, R. (2003). Spontaneous cell polarization through actomyosin-based delivery of the Cdc42 GTPase. Science *299*, 1231–1235.

Wedlich-Soldner, R., and Li, R. (2003). Spontaneous cell polarization: undermining determinism. Nat. Cell Biol. *5*, 267–270.

Wedlich-Soldner, R., Wai, S. C., Schmidt, T., and Li, R. (2004). Robust cell polarity is a dynamic state established by coupling transport and GTPase signaling. J. Cell Biol. *166*, 889–900.

Whiteway, M., Clark, K. L., Leberer, E., Dignard, D., and Thomas, D. Y. (1994). Genetic identification of residues involved in association of α and β G-protein subunits. Mol. Cell. Biol. *14*, 3223–3229.

Whiteway, M. S., Wu, C., Leeuw, T., Clark, K., Fourest-Lieuvin, A., Thomas, D. Y., and Leberer, E. (1995). Association of the yeast pheromone response G protein $\beta\gamma$ subunits with the MAP kinase scaffold Ste5p. Science *269*, 1572–1575.

Winters, M. J., Lamson, R. E., Nakanishi, H., Neiman, A. M., and Pryciak, P. M. (2005). A membrane binding domain in the Ste5 scaffold synergizes with $G\beta\gamma$ binding to control localization and signaling in pheromone response. Mol. Cell *20*, 21–32.